[redacted]

R

LTV RESEARCH CENTER

OTS PRICE

XEROX $ 6.60 ph

MICROFILM $ _____

FINAL REPORT

CONTRACT NO. NASw-647

INVESTIGATION OF BREMSSTRAHLUNG PRODUCED BY THE INTERACTION OF ELECTRONS WITH MATTER

Report No. 0-71000/4R-14

June 1964

W. E. Dance
L. L. Baggerly
N. E. Chappell
B. J. Farmer
J. H. Johnson
D. H. Rester

Approved by: H. B. Gibbons

H. B. Gibbons
Associate Director

TABLE OF CONTENTS

I. INTRODUCTION

The subject of this study is the electromagnetic radiation, or bremsstrahlung, produced when energetic electrons interact with matter in bulk. The energies of the incident electrons ranged from 0.5 to 3.0 MeV - that is to say the electrons had a kinetic energy of the same order as their rest energy. It is in this energy range that our knowledge of bremsstrahlung production is least satisfactory. At non-relativistic energies, where the kinetic energy of the incident electrons is small compared with their rest energy, exhaustive studies, both theoretical and experimental, have been made. (Sommerfeld, Wellenmechanik, Chapter 7). Our knowledge of the characteristics of the bremsstrahlung production at these energies is complete and quantitative. The extreme relativistic case, in which the kinetic energy of the electrons is large compared with their rest energy, has been studied theoretically[1]. Experimental studies are sparse, but tend to indicate reasonable agreement with the theoretical predictions in total intensity, in spectral distribution, and in angular distribution. In the intermediate energy range, experimental data are also slight, and they indicate discrepancies with theoretical estimates in all the pertinent characteristics: total intensity, angular distribution, and spectral distribution. While we share the universal optimism that the basic phenomenon of bremsstrahlung is clearly understood, and the calculations are qualitatively convincing, they remain quantitatively unreliable. The greatest uncertainties are in the energy range from 0.10 to 2.0 MeV. Among the most pertinent studies to date are those carried out at the National Bureau of Standards by Motz and co-workers, who measured bremsstrahlung cross sections for 0.5 and 1.0 MeV electrons on beryllium, aluminum and gold[2]. Their results show the clear need for extending these systematic measurements for these and other materials to higher energies. Moreover, the computation of the bremsstrahlung that would be expected from a thick target is somewhat uncertain, even if one has reliable values for atomic bremsstrahlung cross sections. Such a computation would require knowledge of electron scattering cross sections,

---

1 For an Excellent Survey, see H. W. Koch and J. W. Motz, Review of Modern Physics, 31, 920 (1959)

2 J. W. Motz, Physical Review, 100, 1560 (1955)

and cross sections for energy loss by other means, for which reliable data are not available at this time. Hence, it is also pertinent to measure directly the bremsstrahlung produced by thick targets.

The work described in this report is the initial effort by the Nuclear Sciences Group, LTV Research Center, to fulfill the basic need for experimental bremsstrahlung spectra. The principal research apparatus in this laboratory is a 3.0 MeV Van de Graaff accelerator, equipped to accelerate either positive ions or electrons. A Van de Graaff accelerator lends itself conveniently to the acquisition of bremsstrahlung spectra because of the monoenergetic electron beam, the high degree of stability, and the ease with which the beam energy may be varied - all characteristic of this type of accelerator. Thus the capabilities of this accelerator and associated detection equipment and data handling instrumentation coincide with those required for the urgently needed bremsstrahlung production data.

In the present study radiation intensities were measured from aluminum targets as a function of electron energy, and photon energy and angle of emission, in the electron energy range 0.5 to 3.0 MeV. Bremsstrahlung spectra were accumulated for angles varying from 15° to 120° to the incident beam direction. The electron beam was incident normal to the target, except in the case of photon observation at 90 degrees, in which case the angle of incidence was 45 degrees. Target thickness was varied from 153 $\mu g/cm^2$ for one of the thin targets to 1.9 mg/cm^2 for the thick target bombarded with the maximum energy electrons. The bremsstrahlung pulse height distributions were used to calculate the experimental differential cross sections. These values were compared with the Bethe-Heitler Born approximation cross sections computed from formulas given by Koch and Motz.

It is clear that the production of bremsstrahlung is only one of the interactions of energetic electrons with bulk matter. Others include the scattering of the incident electrons, the production of secondary electrons, the total energy balance between the incident electron and the bulk material (slowing down), and the effects on the bulk material itself. The first of these,electron scattering, is being studied currently in a closely related project in this laboratory.

The results of these basic studies of electron interactions with matter have a number of immediate practical applications. The advent of space flight, with vehicles traveling through regions of high concentrations of energetic electrons and other charged particles, has clearly emphasized the need for reliable data on the secondary radiations produced by these charged particles. Because of its deep penetrating power, bremsstrahlung produced in these interactions is of great importance. Basic measurements of the bremsstrahlung production, along with a knowledge of space electron spectra, are necessary for accurate calculation of radiation doses inside space vehicles. Reliable dose calculations are required both for the assessment of biological hazard, and for the interpretation of instrumental measurements by radiation-sensitive detectors.

The increasing industrial use of electron accelerators, with energies extending into the low relativistic range, also brings with it the need for reliable bremsstrahlung cross section data. This is required for an adequate treatment of shielding of facilities, as well as for prediction of radiation effects on materials subjected to the radiation environment.

II. EXPERIMENTAL METHOD

A. Apparatus

1. General Arrangement

The experimental arrangement for the measurements in the present study is shown in the photograph of Figure 1, and schematically in Figure 2. The electron beam impinges at normal incidence on the target positioned in the center of an evacuated cylindrical chamber. The chamber is mounted at the end of the Van de Graaff accelerator beam drift tube. The bremsstrahlung radiation produced in the target material and emerging at an angle θ to the incident beam direction passes through a thin window in the chamber wall, through two lead collimators, and then through an aperture in the lead sheath enclosing the scintillation spectrometer, where it is detected. A permanent magnet is placed between the two collimators, as shown in Figure 2, to sweep out electrons scattered into the solid angle subtended by the detector. A set of lead inserts for the detector aperture is provided for varying the size of the aperture to obtain the desired count rate in the detector. The defining aperture of the detector is placed at a fixed radius of 98.1 cm from the target, its radius arm being secured to a bearing at a point on the projected axis of the target chamber. The detector carriage can be rotated through a range of angles from 0° to 150° with the target as center. With a one-inch diameter collimator at one meter from the target the detector subtends an angle of 1.5°.

2. Target Chamber

The target chamber used in the initial measurements was fabricated from lucite (Figure 3), chosen for its low effective atomic number so as to minimize background radiation from the chamber contributed by bremsstrahlung resulting from scattered electrons. The chamber was constructed from lucite tubing 12-inches in diameter by 11 inches long by 1/4-inch wall. The end plates were cut from 1 inch lucite sheet. Either the target, or a beam-viewing quartz disc can be positioned remotely in the beam. The position of the target is observed by a television monitor. The windows for bremsstrahlung observation are of .005" mylar, bonded to the outside of the chamber

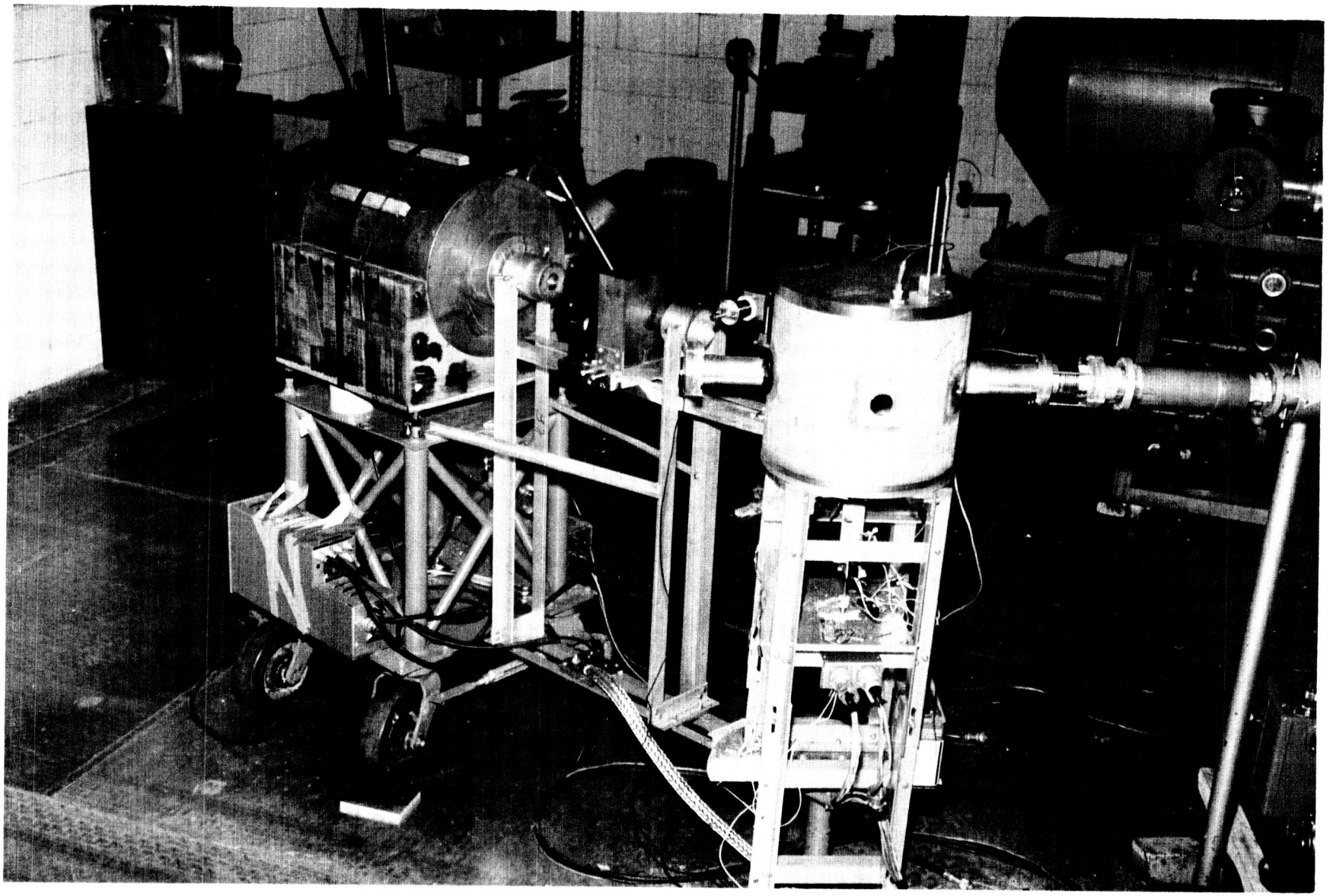

Figure 1. Experimental Arrangement for Bremsstrahlung Measurements

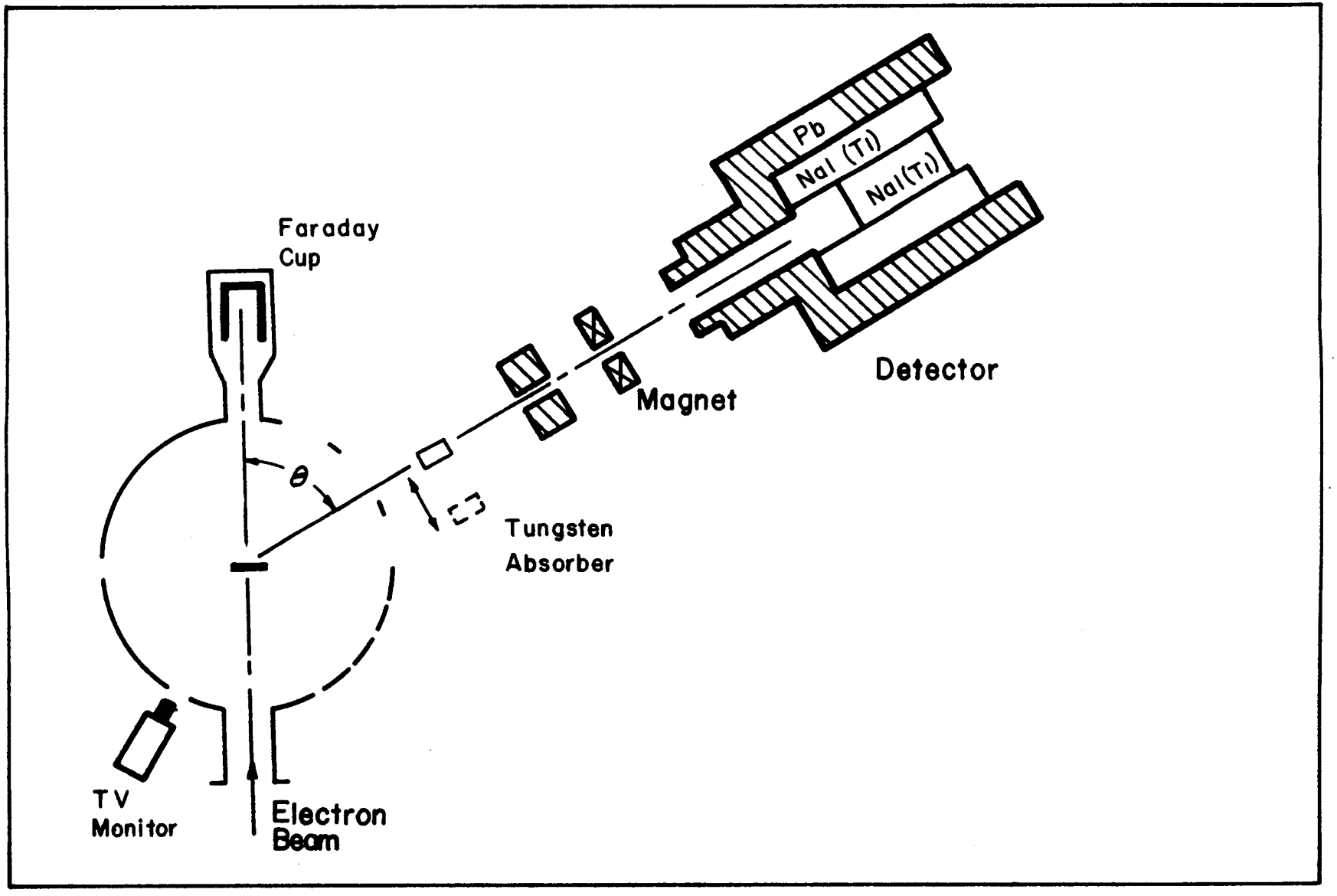

Figure 2. Schematic of Experimental Arrangement

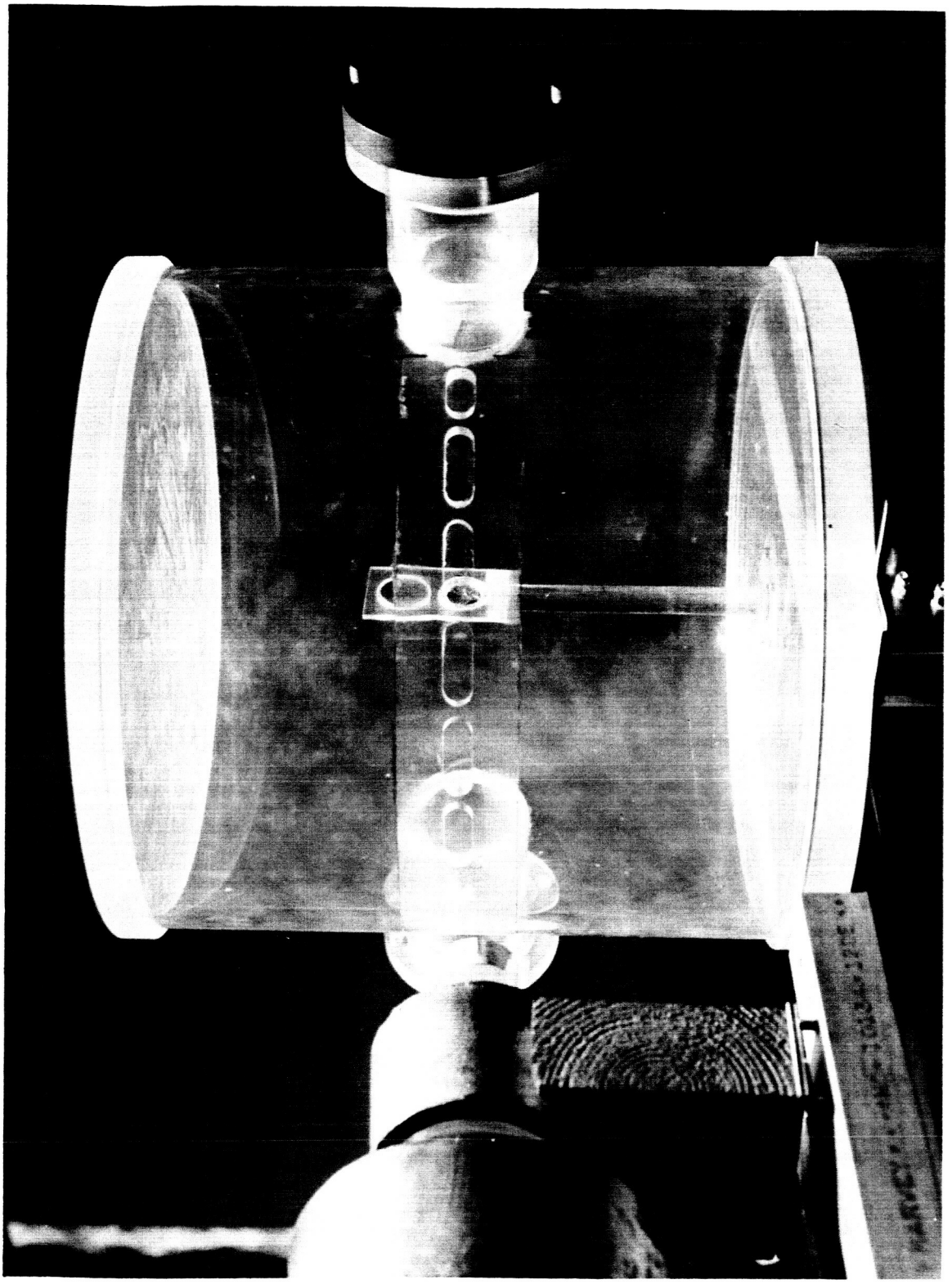

Figure 3. Bremsstrahlung Target Chamber used for Initial Runs

wall with Epibond 101* cement. With these windows, absorption of the X-radiation is less than one percent at photon energies above 20 keV.

At a later stage in the measurements the lucite chamber was replaced with an aluminum one, due to the difficulty in obtaining accurate electron current integration using the lucite chamber (as described below). The aluminum chamber was identical in geometry to the original chamber.

3. Electron Beam Current Integration

For determining the number of electrons incident on the target during a run, the initial chamber was fitted with a 2-inch Faraday Cup of graphite. This was separated from the chamber by a 66-inch long exit tube and shielded with sufficient thickness of lead to minimize this source of background radiation.

During the thin target bremsstrahlung measurements, when the target is in the beam, an appreciable portion of the incident beam is scattered, and not collected by the Faraday cup. It is necessary, then, to determine the ratio of the current collected with the target in place to the total beam current, i.e., that collected with the target removed. This procedure, while simple in concept, proved very tedious in practice. Furthermore, the repeatability of this measurement was poor - sometimes no better than 20 - 25 percent. It was thought that this unreliability might be due to an electrostatic charging of the lucite walls. However, coating the inside of the chamber with a conducting layer of aquadag did not improve the situation significantly. It was for this reason that a new target chamber of aluminum was built.

The aluminum chamber also has a graphite beam stop on the side opposite the beam entrance. The chamber is electrically insulated from ground, and all the current collected on the beam stop, chamber, and target is integrated. This has resulted in a much more reliable measure of the incident beam current. There is no detectable difference in the collected beam when the target is in or out of the beam.

---

* Furane Plastics, Inc.

It was expected that the aluminum chamber would produce a higher background radiation than the lucite one, because of its higher effective atomic number. However, the background increased by only about 10%, and this background was further reduced by appropriate placement of lead shielding.

To prevent backscattered electrons from escaping through the entrance tube to the chamber, a repelling voltage of -300 V was applied to a short section of the beam tube, electrically isolated from the chamber and from the grounded portion of the accelerator drift tube. The biased section was provided with a 7/8" diameter carbon aperture to decrease the solid angle subtended by the entrance port. Target currents in the range 10^{-9} to 10^{-7} ampere were measured with $\frac{1}{2}$% accuracy with an Elcor Model A309A current integrator. In the range from 10^{-10} to 10^{-9} ampere, currents were measured with a Keithley electrometer Type 600A, the output of which was fed into the current integrator. Stability of the target current during runs was about 20%, and the zero target current setting was checked at frequent intervals.

4. Electron Beam Stabilization

When the Van de Graaff generator is used to accelerate positive ions, the source of these ions is a gas discharge r.f. ion bottle. If it is desired to accelerate electrons, one can either extract electrons from this same ion source, or replace the r.f. ion source by a heated filament. Further, the focussing characteristics of the accelerating column is slightly different for electrons and for positive ions. The complete conversion of the accelerator from operation with positive ions to operation with electrons only is a considerable modification. There are some substantial advantages to be gained by retaining the positive ion capability - not the least of these being the ease of making periodic checks of the accelerator energy calibration by (p,n) threshold and (p,γ) reaction measurements.

For these reasons, during the early portion of this work considerable effort was directed toward using the r.f. ion source and positive ion accelerating column for accelerating electrons. However, the quality of the resulting beam, particularly in its focus and alignment, was not satisfactory. Consequently, the accelerator was converted to incorporate the electron filament source, and the electron accelerating column.

After acceleration, the electron beam is deflected through an angle of 25° by an analyzing magnet and passes through a pair of carbon control slits before it strikes the target. The total flight path from the accelerator to the target is 26.5 feet. The function of the control slits is to maintain the beam on the target. The two slits are connected to the input of a difference amplifier, the output of which controls the current through the deflection magnet. Thus, if the beam wanders to one side, a correction signal is sent to the deflection magnet to return the beam to its central position.

At extremely low beam currents, below about 10^{-9} amp, the portion of the beam collected by the control slits is too small for proper control of the beam. For operation at these low currents, an auxiliary pair of slits is formed by a pair of plastic scintillators, viewed by photomultipliers. The outputs of the photomultipliers then are taken to the input of the control difference amplifier. With this technique, beam currents as low as 10^{-12} amp have been effectively controlled.

Over the long flight path of the electron beam used in this experiment, the deflection of the beam due to the earth's magnetic field is not negligible-- at 0.5 MeV, it amounts to almost 15 cm! To avoid such deflection, the entire beam tube was enclosed in a magnetic shield of "Conetic" metal.

5. Detector

The scintillation spectrometer is of the dual crystal anticoincidence type introduced by Trail and Raboy[3]. The detector is a 2.32 by 6 inch NaI(Tl) crystal surrounded by a NaI(Tl) annulus, 8 inches in diameter and 12 inches long. This assembly is enclosed by a 3-inch thick lead sheath. The detector arrangement is seen in the photograph of Figure 4. Figure 5 is a block diagram of the associated electronic circuitry, and Figure 6 shows the preamplifier assembly. The dual crystal arrangement affords a substantial reduction in room background as well as in background due to Compton scattering and pair production in the center crystal. Bremsstrahlung reaching the center

---

3 C. C. Trail and Sol Raboy, Reviews of Scientific Instruments, 30, 425 (1959)

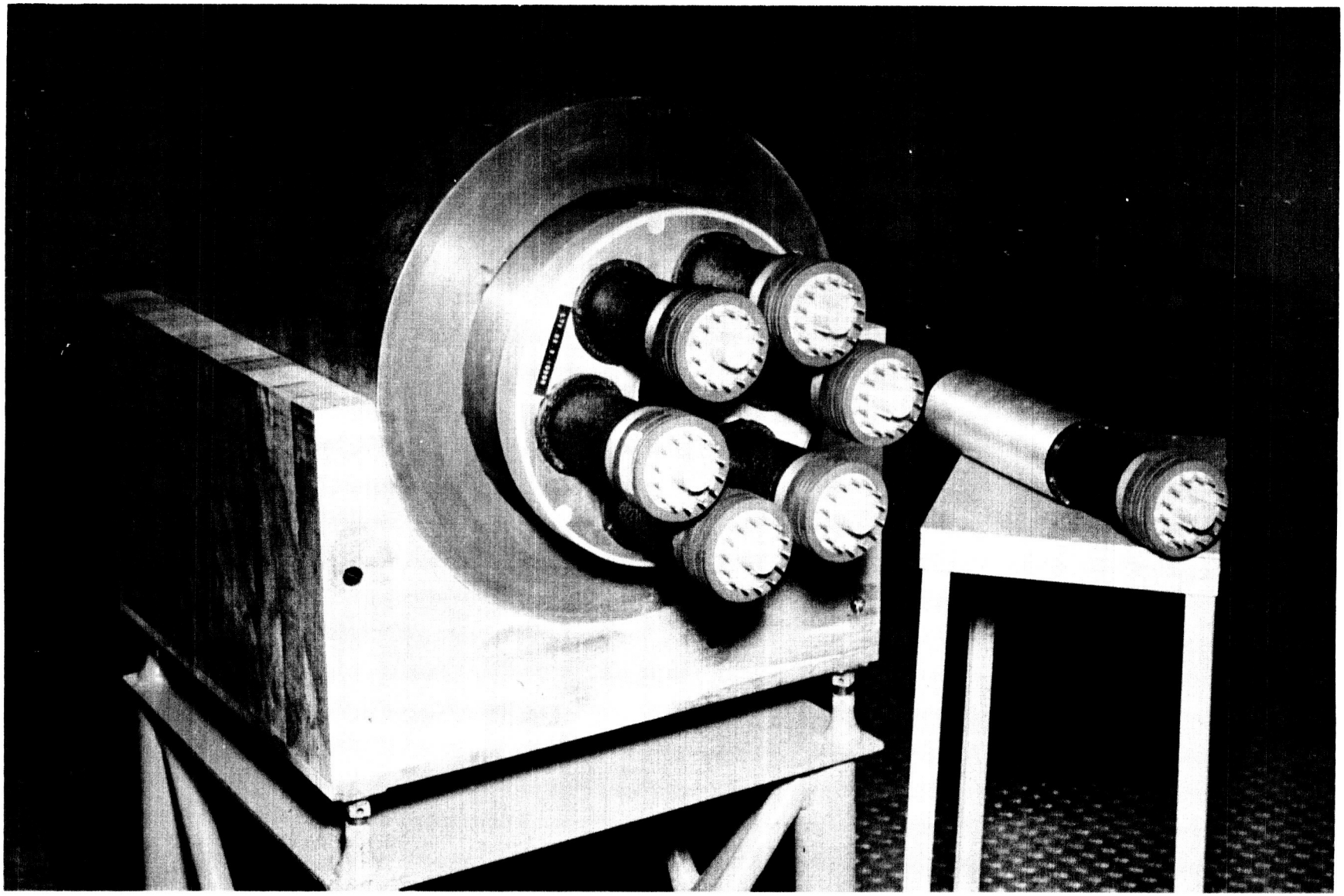

Figure 4. NaI(Tl) Dual-Crystal Anticoincidence Spectrometer Assembly

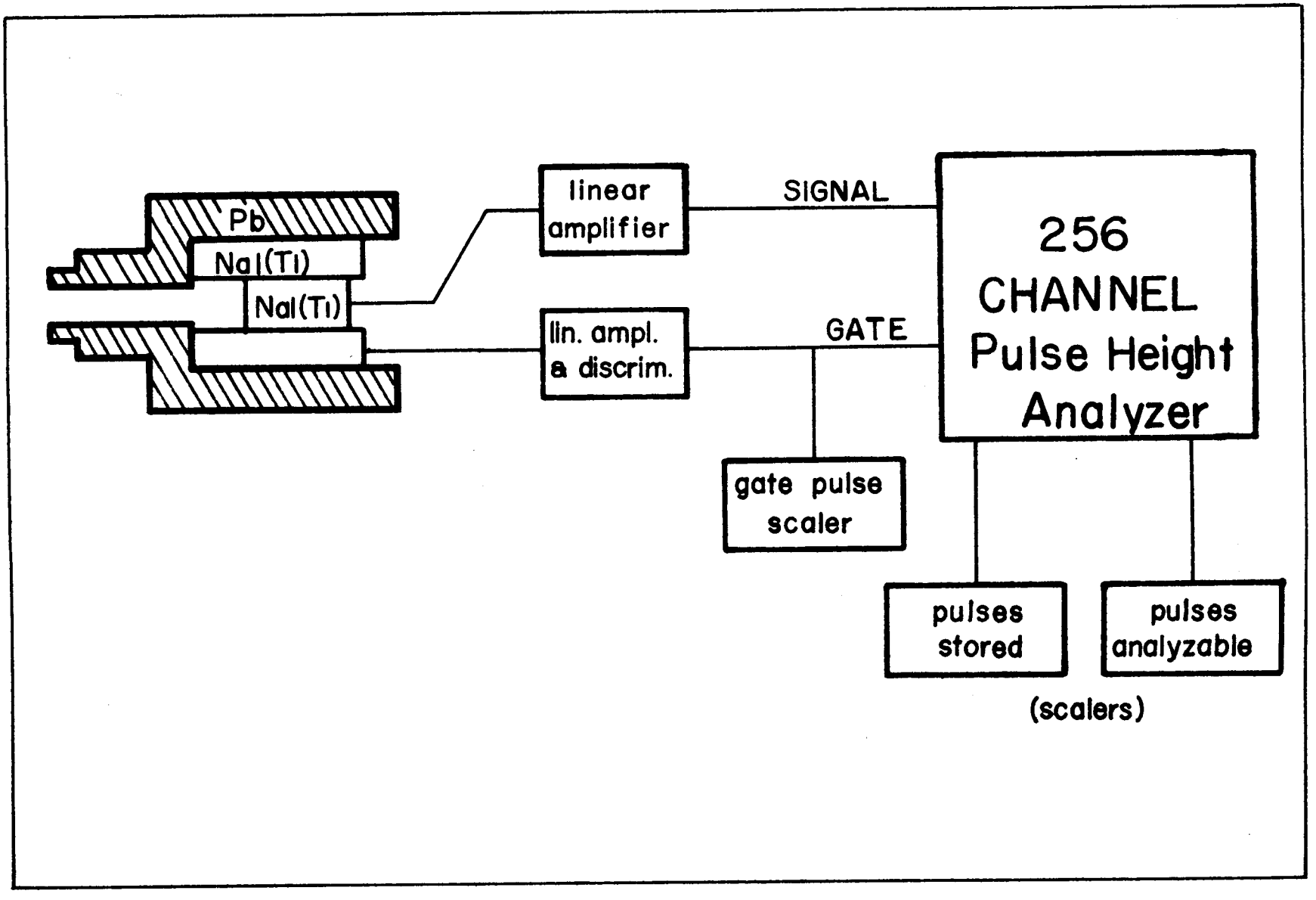

Figure 5. Block Diagram of Spectrometer and Associated Electronic Circuitry

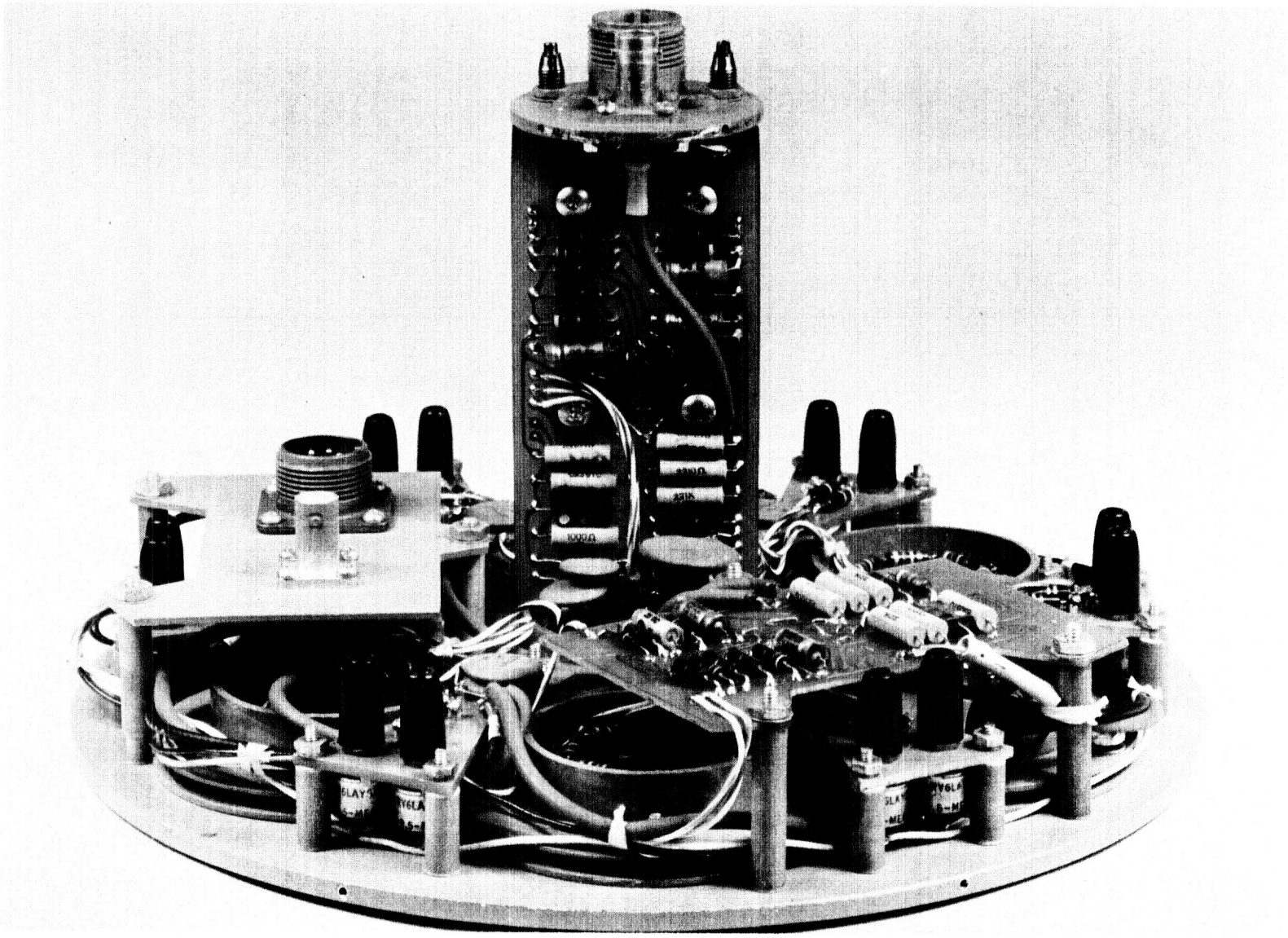

Figure 6. Dual Preamplifier Assembly for Anticoincidence Spectrometer

crystal is collimated by the lead sheath, and if the full energy is not absorbed in the center detector, the pulse from the outer crystal corresponding to partial absorption in that crystal is used in an anti-coincidence mode to gate off a pulse height analyzer. Figure 7 shows the .511 and 1.277 MeV gammas from ^{22}Na analyzed with this spectrometer. Comparison of the gated and ungated spectra shows a significant reduction in the Compton background and suppression of the one-escape and two-escape peaks. Light from the center crystal is viewed by an RCA 5342A photomultiplier tube, while the annulus is viewed by six of these tubes. The signal from the center detector is amplified by the linear amplifier (RCL Model 20509) located on the detector carriage, and subsequently fed into an RCL Model 20617 256-channel pulse height analyzer. The lower level and base line discriminators in the 256-channel analyzer were set for analysis of pulses whose heights correspond to energies greater than 20 keV. The gate signal derived from the NaI annulus is fed into another RCL Model 20509 single channel analyzer. This analyzer puts out a 7 μs blocking gate pulse each time it receives an input pulse corresponding to an energy greater than 40 keV.

The live time correction factor for the multichannel analyzer was determined by taking the ratio, for a given run, of the total number of pulses stored in the analyzer to the total number of analyzable pulses arriving at the analyzer. The analyzable pulses are those with pulse heights between those of the lower level and upper level discriminator settings on the analyzer. These pulses are counted separately by a fast scaler (RCL Model 20322). An additional live time correction was applied to account for the 7 μ sec dead time per gate pulse to the gating circuit in the analyzer.

B. Targets

The material chosen for the initial measurements was aluminum. For thin target measurements a target is classified as thin if the electron scattering and energy loss in the target have a negligible influence on the energy and angular distribution of the bremsstrahlung. This condition pre-supposes, therefore, that for a very thin target only single scattering of the electrons occurs. A convenient expression for determining the angular spread of the electrons emerging from the target is given by Blanchard[4], from multiple

[4] C. H. Blanchard, National Bureau of Standards Circular 527, 9 (1954)

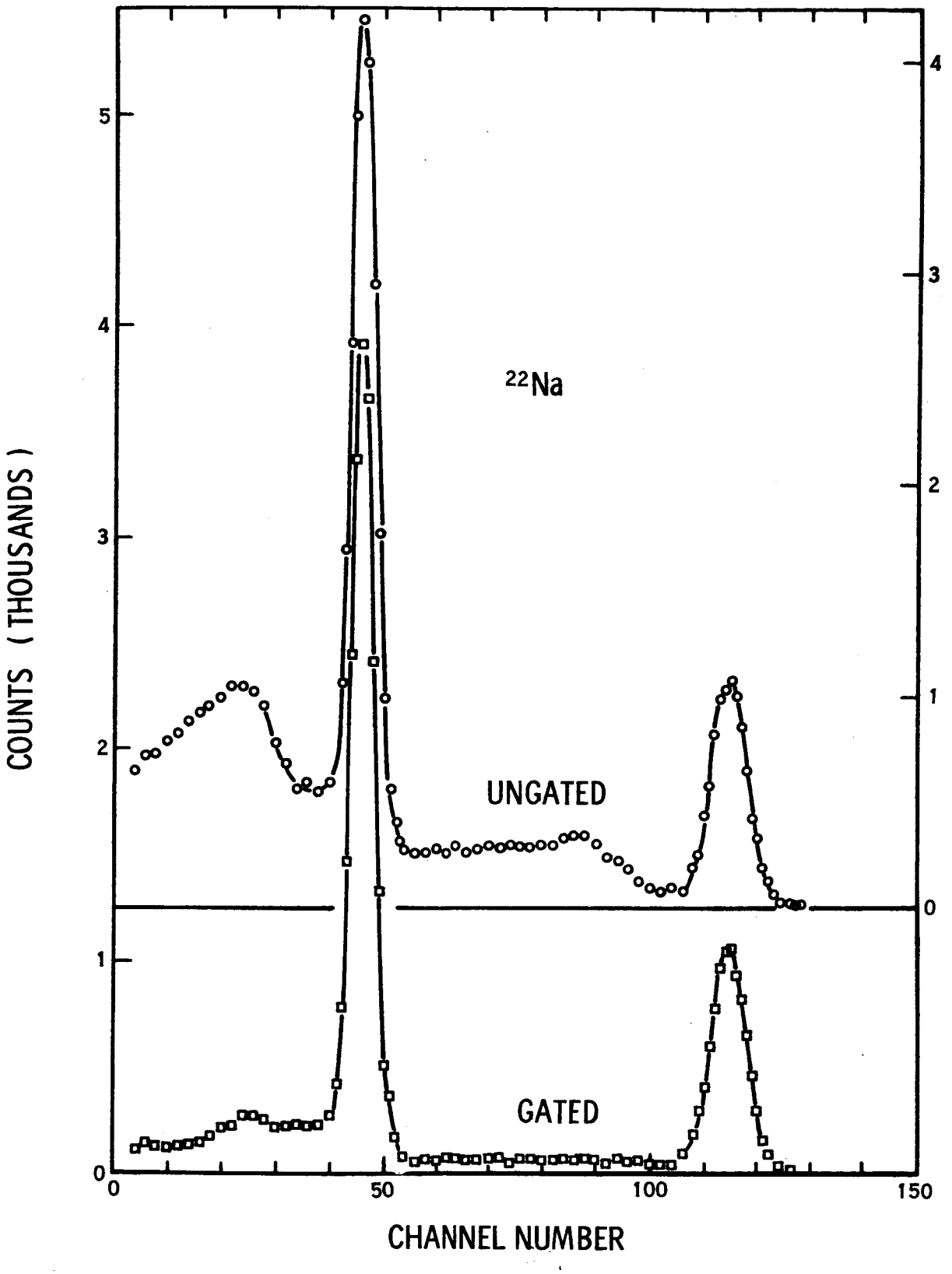

Figure 7. ^{22}Na Pulse Height Distribution in the Anticoincidence Spectrometer Showing Effectiveness of Gating in Background Removal

scattering theory:

$$\langle \alpha^2 \rangle_{av} \approx 0.6\, Z\, \bar{\Delta}/T_o\, (T_o + 1)\,,$$

where $\bar{\Delta}$ is the average energy loss in the target, T_o is the initial kinetic energy in MeV, and $\langle \alpha^2 \rangle_{av}$ is the mean square angle of emergence of the electrons from the target. Target thicknesses in this study were selected according to the criterion used by Motz and Placious[5]:

$$1 - \langle \cos \alpha \rangle_{av} \approx \langle \alpha^2 \rangle_{av}/2 = 0.02.$$

The thick target data were obtained with samples of infinite thickness, i.e., of thickness equal to or greater than the maximum range of electrons in the target material.

Three of the thin targets were prepared from rolled aluminum foil, supplied by the Alcoa Research Laboratory, Fabricating Metallurgy Division. These foils have thicknesses of 20.56 mg/cm^2, 7.26 mg/cm^2, and 3.56 mg/cm^2, corresponding to nominal thicknesses of 0.003", 0.001", and 0.0005", respectively. Seven other targets ranging in thickness from 83 to 890 micrograms/cm^2 were prepared by vacuum evaporation of pure aluminum wire. The technique used was that described in several reports from Lawrence Radiation Laboratory[6]. Briefly, the method used for evaporation of the aluminum targets is as follows: A glass microscope slide is dipped into a dilute solution of detergent and sugar, thus providing a water-soluble film on the glass. The slide is placed on top of an accurately measured mask in a vacuum chamber, and aluminum is evaporated from a tantalum boat[7]. The glass slide is slowly immersed at a shallow angle in water, dissolving the substrate and allowing the thin aluminum film to float off on the surface of the water. The thin film is picked up on a piece of velvet cloth, washed, dried, and weighed. For a

---

5 J. W. Motz and R. C. Placious, Physical Review 109, 235 (1958)

6 W. F. Brummer and H. G. Patton, UCRL-6225, 1961; UCRL-6382, 1961; M. A. Williamson, UCRL-6989, 1963.

7 L. Holland, Vacuum Deposition of Thin Films, John Wiley, N. Y. (1956)

self-supporting target the film is then attached with cement to a mounting ring. The thickness of the films was determined by weighing, assuming that the thickness is uniform over the surface. The uniformity and an independent measure of the thickness were determined by the absorption of monoenergetic alpha particles. The accuracy of the determination is from ± 3 to ± 5 micrograms/cm^2 for the evaporated targets, and ± 0.2% for the rolled foils.

The thick targets were prepared from 99.99% pure aluminum sheet, supplied by Reynolds Aluminum Company. Two thicknesses were used: .080" and .274", for the energy ranges 0.50 - 1.00 MeV and 2.00 - 3.00 MeV, respectively.

C. Calibration Procedures

1. Calibration of Detector Efficiency

To obtain accurate bremsstrahlung spectra, it is necessary to know the spectral response of the detector for photons of various energies. It is thus necessary to answer the following question: if N photons of energy E are emitted at the target position, how many pulses of height H will be recorded by the detector system? The answer to this question will involve three distinguishable factors:

1. geometrical factor - the solid angle subtended by the detector at the target position,
2. absorption between the source and detector, and
3. intrinsic response of the detector.

These factors will be considered in turn.

Geometrical Factor:

As described previously, photons from the target pass through an opening in a lead collimator, then through a defining lead aperture immediately in front of the detector. The diameter, d, of this aperture was measured by a micrometer, and the distance, L, from the target position was measured with a meter stick and two plumb bobs. The solid angle of this aperture was then simply computed:

$$d\Omega = \frac{\pi d^2}{4L^2}$$

The two apertures used had nominal diameters of $\frac{1}{2}$ inch and 1 inch. The corresponding solid angles were $(1.31 \pm .01) \times 10^{-4}$ and $(5.42 \pm .04) \times 10^{-4}$ steradian, respectively.

Absorption:

Between the target and the scintillation crystal, a photon must pass through 0.005 in. of Mylar, 98 cm of air, and the materials on the front face of the crystal. The crystal is secured around the edge of the face, leaving a thin window $1\frac{3}{4}$" in diameter. The window consists of 34.1 mg/cm^2 of aluminum and 20 mg/cm^2 of aluminum oxide. The computed transmission of these absorbers as a function of energy is summarized in Figure 8. Note that the absorption is less than 3% for photons with energies greater than 100 keV. Below this energy, the absorption increases but remains less than 10% down to 30 keV. It should be noted that although the thin window covers only approximately half the surface of the front face of the crystal, this did not restrict the detector in this experiment, as the lead collimators used had diameters of 1" and $\frac{1}{2}$".

Intrinsic Response:

The response of the detector to monoenergetic photons is shown in Figure 9. The shape is reasonably well approximated by a gaussian, centered at the photon energy, and a low energy tail. The approximation used for the tail is rectangular at low energies, and triangular under the photopeak. The photopeak efficiency is taken to be the total number of counts in the gaussian portion of the curve divided by the number of photons which get into the crystal. To describe the crystal response in this approximation, it is sufficient to know three parameters: the gaussian portion is described by the photopeak efficiency (area under the gaussian) and the full-width-at half-maximum; the tail portion is then described by the ratio of the height of the tail to the area of the gaussian portion, in counts per MeV per photopeak count. These parameters were measured for several monoenergetic gamma rays from standard radioactive sources. The particular sources used, with the energies of their gamma rays in parentheses, were:

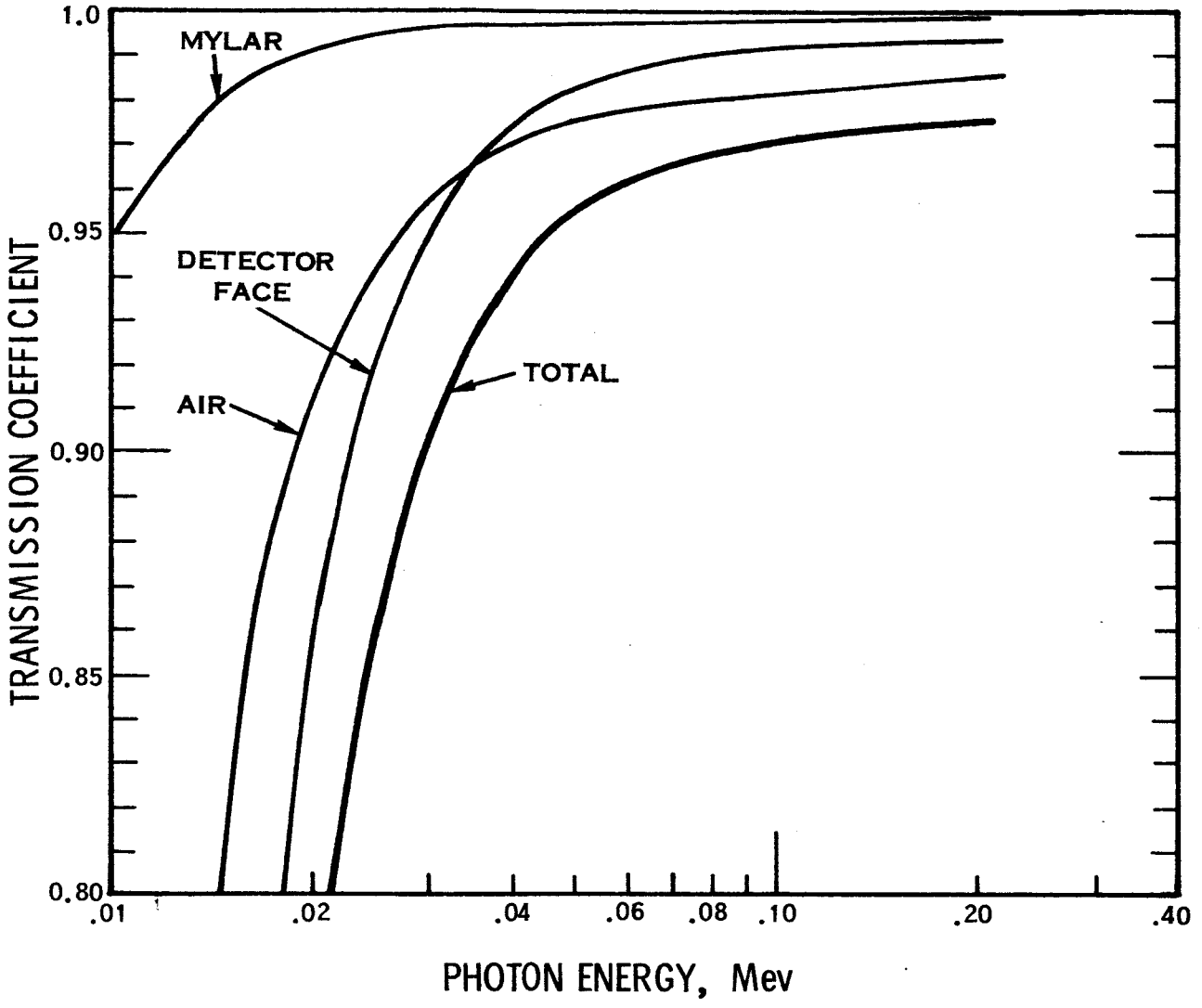

Figure 8. Gamma-ray Transmission of Various Materials Between Target and Detector

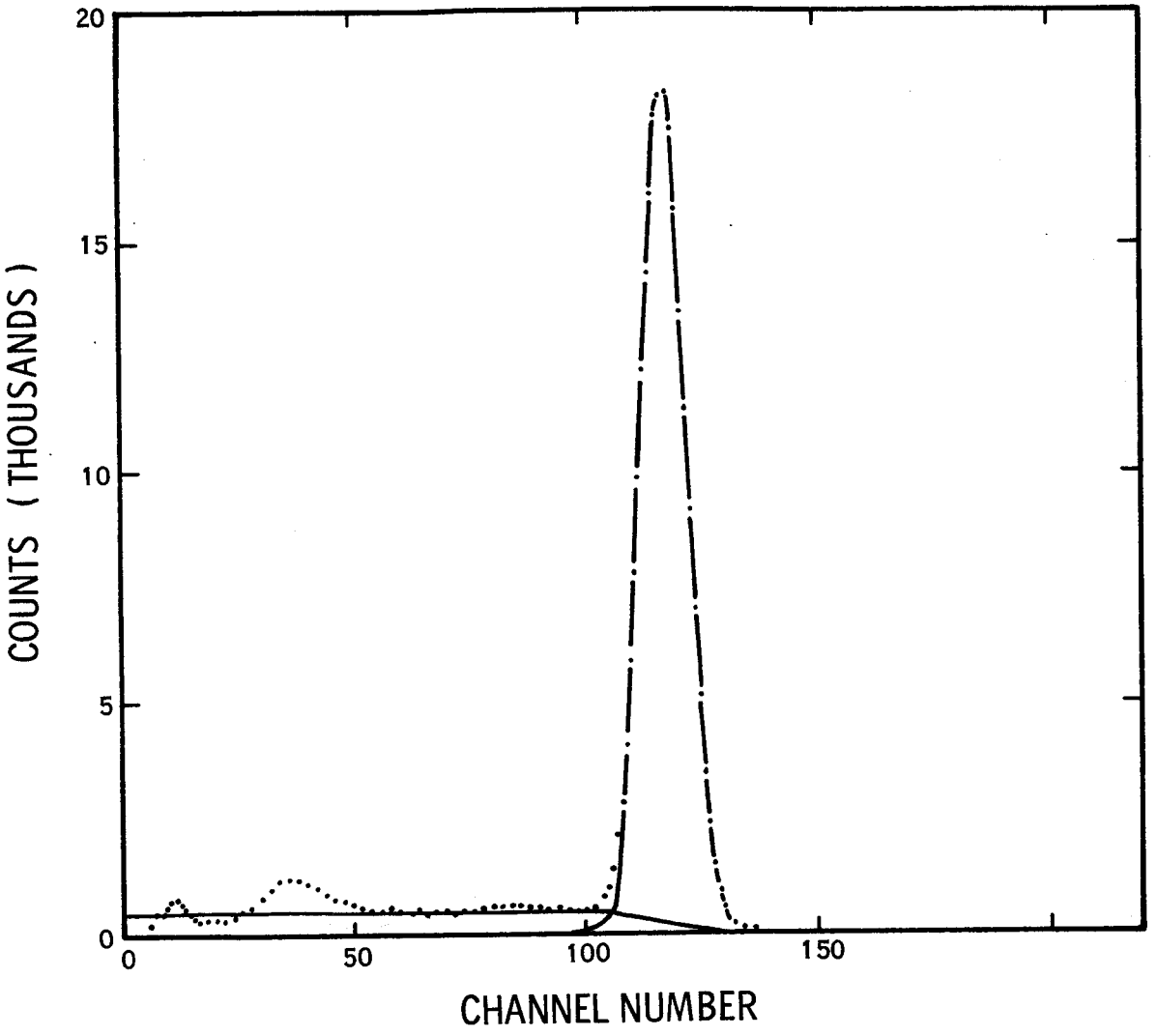

Figure 9. Response of Spectrometer to Gamma Rays from ^{137}Cs, Showing Gaussian and Tail Portions

^{22}Na (0.511, 1.277)[1]

^{137}Cs (0.662)[2]

^{54}Mn (0.834)[3]

^{88}Y (0.898, 1.837)[3]

^{60}Co (1.173, 1.333)[4]

^{24}Na (1.367, 2.754)

[1] Supplied by Minnesota Mining and Manufacturing Co.

[2] Supplied by Nuclear Chicago Corp.

[3] Supplied by Nuclear Science and Engineering Co.

[4] Supplied by Isotope Specialties Co.

In each case except ^{24}Na, the activity of the source was specified by the supplier. The sources were placed at the target position, and a spectrum accumulated for a fixed time. The resulting spectrum was then fitted, over a narrow range of channels including the photopeak, with a curve of the form

$$N(C) = A_1 + A_2C + A_3 \exp\left[-(C - A_4)^2/2A_5^2\right],$$

where C = channel number, and N(C) = number of counts per second in Channel C.

The parameter A is proportional to the full-width-at-half-maximum (fwhm = 2.354 A_5), and the number of counts in the gaussian portion of the peak is proportional to the product of A_3 and A_5 (area = $\sqrt{2\pi}\ A_3\ A_5$).

The range of calibration was extended upward using an uncalibrated source of ^{24}Na. Using this source, the ratio of efficiencies at 1.367 and 2.754 MeV was determined. The efficiency at the lower energy was found by interpolation, thus fixing the efficiency at the higher energy.

The photopeak efficiency, corrected for absorption, is shown in Figure 10.

The resolution (fwhm/photon energy) is shown in Figure 11. The

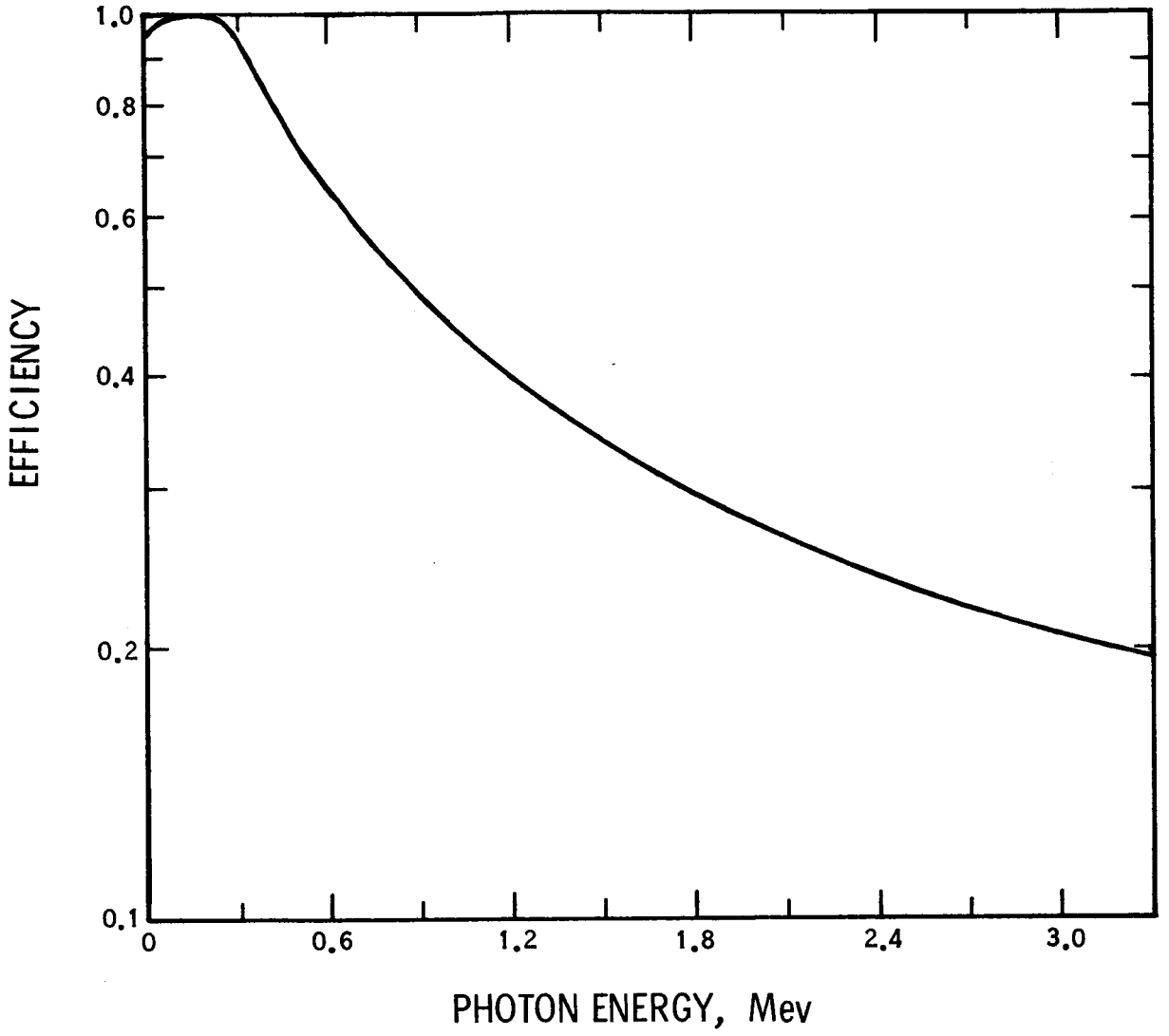

Figure 10. Photopeak Efficiency of Spectrometer

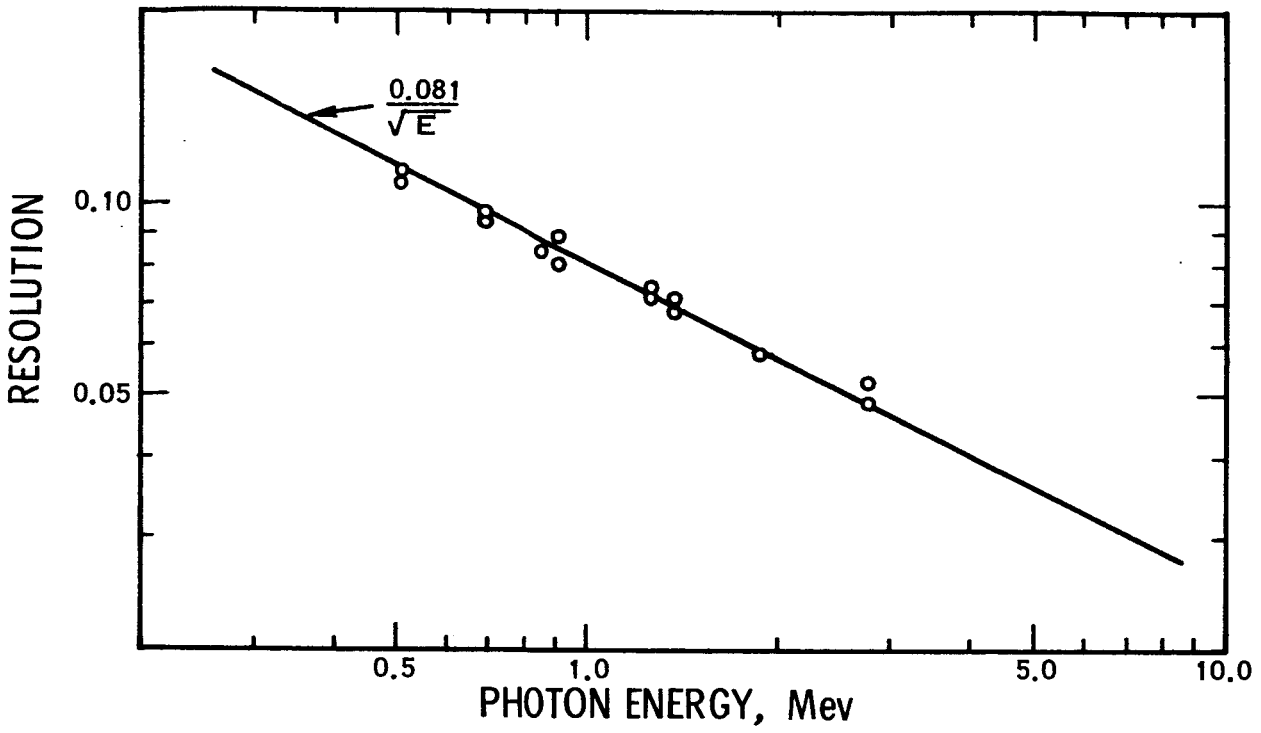

Figure 11. Spectrometer Resolution

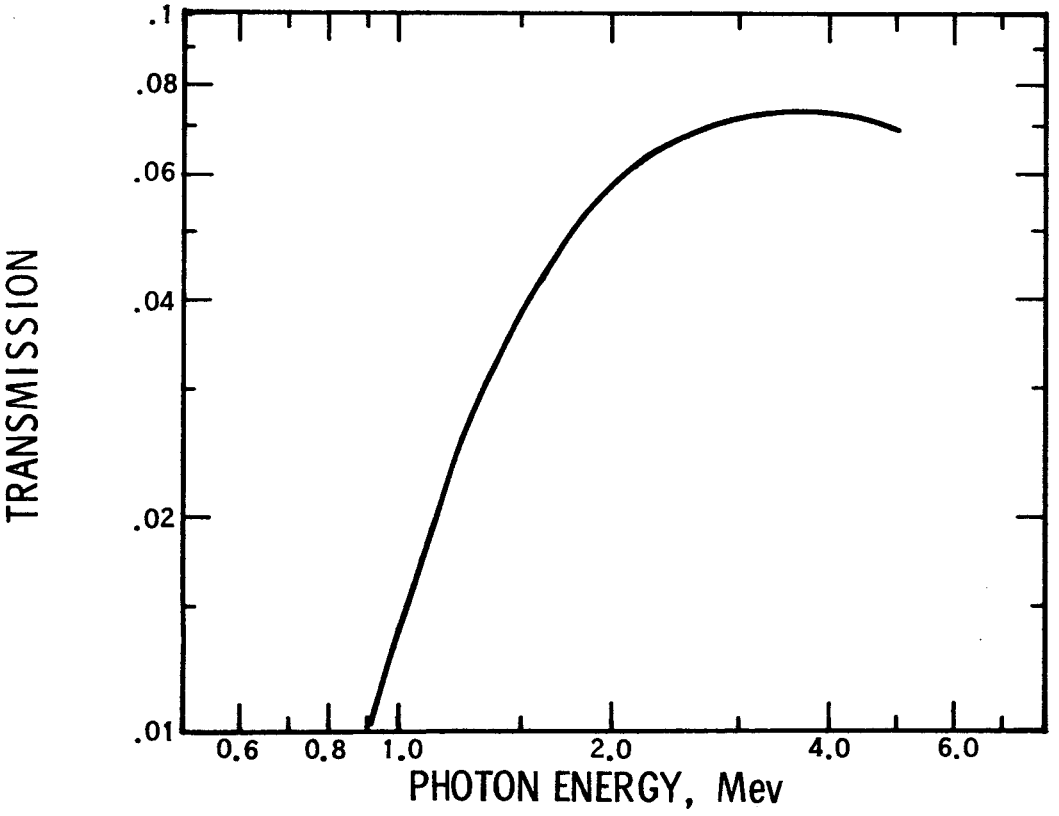

Figure 12. Transmission of Tungsten Absorber as a Function of Photon Energy

straight line on this figure has the slope 0.5, indicating that the resolution is well approximated by

$$\text{Res.} = 0.081\ (E)^{-\frac{1}{2}} \quad ,$$

where E is the photon energy in MeV.

2. Correction for Method of Subtracting Background

When compiling a bremsstrahlung spectrum, a certain number of photons are counted which do not come from the target. To subtract this unwanted background, a tungsten absorber is placed directly between the target and the detector. This blocks the radiation which comes from the target region (see arrangement, Figure 2). In this fashion, a "background spectrum" is accumulated, which is then subtracted from the first spectrum (after normalization to the same integrated beam and correction for analyzer dead time). At high photon energies the tungsten absorber is not totally opaque - the transmission is almost 8.5% at 3.0 MeV, and about 1.5% at 1.0 MeV. Thus, a portion of the desired spectrum is accumulated along with the background, and subtracted from the spectrum. A correction factor for this must be added. If T(E) is the transmission of the tungsten absorber for photons of energy E, the number of counts in the spectrum at this energy, after background subtraction, should be multiplied by the factor

$$(1 - T(E))^{-1} \quad .$$

The transmission as a function of energy is shown in Figure 12.

3. Energy Calibration of Detector

Before each bremsstrahlung spectrum is accumulated, a calibration spectrum is taken, using either the 0.511 and 1.277 MeV gamma rays of ^{22}Na, or the 0.898 and 1.837 MeV gamma rays of ^{88}Y, or both. The photopeaks of the calibration spectra are fitted with a curve of the form

$$N(C) = A_1 + A_2C + A_3 \exp\left[- (C - A_4)^2/2A_5^2 \right] \quad ,$$

as before. The parameter A_4 then identifies the channel number which corresponds to the energy of the gamma rays. With two or more such points, a linear relation between analyzer channel number (i.e., pulse height) and energy can be established. This relation was calculated by the computer, which then used

the linear function to identify an energy with each channel number.

4. Electron Beam Energy Calibration

The energy of the electron beam was calibrated using a lithium-drifted silicon detector prepared in this laboratory. The potential on the accelerator high voltage terminal was measured with the generating voltmeter read by a Hewlett-Packard Model 412A VTVM. The solid state detector, which was cooled to -80°C was placed at the end of the beam tube at the position normally occupied by the Faraday cup, and the peak in the pulse height spectrum due to the electrons scattered from the thin target foil was observed. Energy calibration of the detector was achieved by reference to the internal conversion electron line from Cs^{137}. In this detector the K- and L-conversion lines at .625 and .657 MeV are well resolved, as seen in Figure 13. After applying a correction for energy loss in the target, the correlation of incident electron-beam energy to voltmeter reading is thus established. The accuracy of the beam energy determination is estimated to be approximately ± 15 keV.

5. Spectrometer Angle Calibration

Calibration of the protractor measuring the detector angle was performed as follows: A transit centered over the target was used to sight on a plumb line dropped to a quartz beam viewer located at the end of an extension to the exit tube of the target chamber. By observing the position of the electron beam spot at the quartz viewer, the 0° beam position was established. Another plumb line at the center of the detector, aligned by removing the center crystal of the spectrometer and sighting down the hole at the target, served for determining other angles in the calibration of the protractor. The precision of the angular measurement of the detector position is ± 0.2°.

D. Data Processing

A program was written for the IBM 7090 computer which takes as inputs the laboratory data, and produces as outputs the bremsstrahlung yield and reduced intensity. The input data includes:

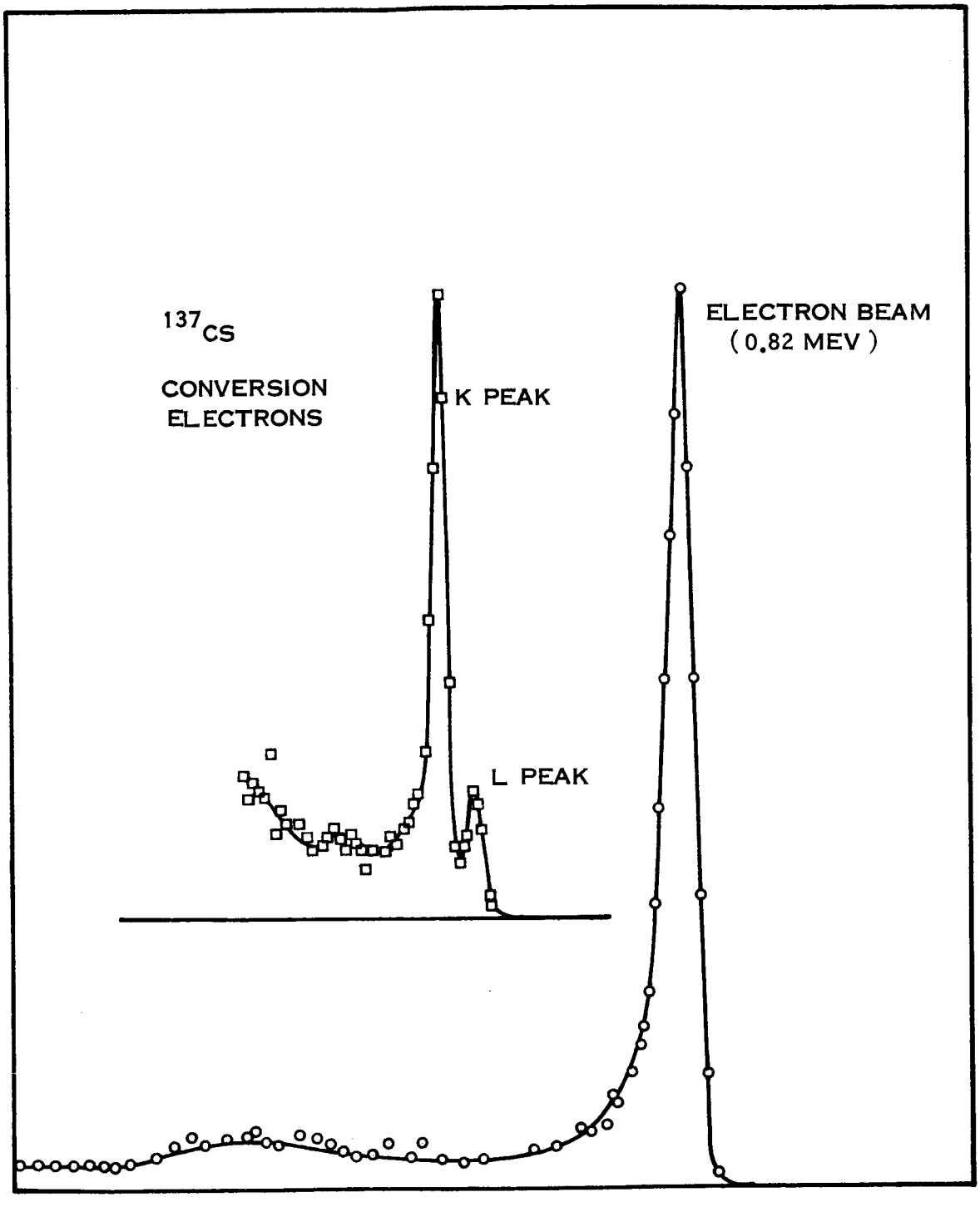

Figure 13. Electron Beam Energy Calibration

Symbol		Meaning
1.	$N_A(C)$	Main spectrum, number of counts in channel C of pulse height analyzer
2.	$N_B(C)$	Background spectrum - same form as $N_A(C)$
3.	$N_{cal}(C)$	Calibration spectrum
4.	I_A	Total charge incident on the target during accumulation of main spectrum, in coulombs
5.	I_B	Total charge incident on target during background run
6.	$LT_A(LT_B)$	Analyzer live-time fraction for main (background) spectrum
7.	$d\Omega$	Solid angle subtended by detector at target, in steradians
8.	dX	Target thickness (for thin-target bremsstrahlung data), in mg/cm^2
9.	$\epsilon(K)$	Corrected photopeak efficiency of detector, as a function of photon energy
10.	$R(K)$	Resolution of detector at photon energy K
11.	$H(K,K')$	Low-energy-tail portion of detector response, at pulse height K due to photons of energy K'.

The computer first corrects the main spectrum and the background spectrum separately for live time and reduces each to unit charge (1 electron) and then subtracts the background from the main spectrum. This result is then divided by the solid angle of the detector, to produce a normalized net spectrum,

$$G(C) = \frac{e}{d\Omega} \left[\frac{N_A(C)}{(LT_A)(I_A)} - \frac{N_B(C)}{(LT_B)(I_B)} \right] \quad \frac{\text{counts}}{\text{channel-steradian-electron}}$$

Next, using the calibration spectrum, the independent variable is changed from channel to photon energy K. This spectrum is then divided, point by point, by the efficiency of the detector, to produce the first approximation

to the experimental bremsstrahlung yield. If dK/dC is the energy increment corresponding to one channel, then

$$F(K) = \frac{G(C)}{[dK/dC][\epsilon(K)]} \qquad \frac{\text{photon}}{\text{MeV - steradian - electron}}$$

This spectrum is then corrected for the line-shape of the response of the detector. The result of this final computation is then printed out as the bremsstrahlung yield

$$\frac{dn}{dK\ d\Omega} .$$

It is also convenient to have the intensity of bremsstrahlung produced - which is the product of the number of photons and the energy/photon, K. To facilitate comparison with results from other materials, this is divided by the square of the atomic number, and the "reduced intensity", or

$$\frac{K}{Z^2} \quad \frac{dn}{dK\ d\Omega}$$

is printed out.

III. RESULTS

The measured values of bremsstrahlung reduced intensity, from a thick aluminum target, are presented in Figures 14 through 18, and in Tables 1 through 25. The reduced intensity,

$$\frac{K}{Z^2} \quad \frac{dn}{dK\, d\Omega}$$

has the units $(\text{steradian})^{-1}\ (\text{electron})^{-1}$. Also presented in the tables are the corresponding values of the photon yield, $dn/dk d\Omega$, which has the units $\text{photon}\ (\text{MeV})^{-1}\ (\text{steradian})^{-1}\ (\text{electron})^{-1}$.

The target thickness was 0.584 gm/cm^2 for the 0.50, 0.75 and 1.00 MeV data. This just exceeds the residual range for 1.00 MeV electrons[8]. For measurements at 2.00 and 3.00 MeV, the target had a thickness of 1.878 gm/cm^2, which just exceeds the residual range for 3.00 MeV electrons.

For angles other than 90°, the target was normal to the incident electron beam. For the case of photons emitted at 90°, the target was placed at 45° to the incident electron beam, with the spectrometer viewing the side opposite the incoming beam. Thus, the bremsstrahlung was transmitted through the target before being detected. Only for $\theta = 120°$ was the spectrometer on the same side of the target as the incident beam.

From the graphical presentations it can be seen that:

(1) The reduced intensity is a smoothly decreasing function of photon energy at all angles.

(2) There is the expected peaking at small angles, the tendency being more pronounced at higher electron energies. This forward peaking is also more pronounced at photon energies near the upper limit. For example, for $T_o = 2.0$ MeV, at $K = 1.8$ MeV, the intensity at 15° is 107 times that at 90°, while at $K = 0.5$ MeV, the corresponding ratio is only 11.

---

8 L. V. Spencer, Physical Review, 98, 1595 (1955)

(3) At backward angles (120°) the reduced intensity as a function of the ratio K/T_o is almost independent of T_o. At 60° and 90°, the reduced intensity as a function of K/T_o approaches the same value, independent of T_o, for $0.8 < K/T_o < 1.0$. At smaller values of K/T_o, the yield increases with increasing electron energy, T_o.

(4) There appears to be a depression in each of the curves. It will be noticed that this depression occurs at a photon energy of about 275 to 300 keV, independent of both T_o and angle. This leads to the strong presumption that the source of this depression may lie in the detecting system - that is, that it is not real. One possibility that would make this presumption plausible is that the efficiency of the detector in this energy range was deduced by interpolation from reliable points at energies of 200 keV and 511 keV. If the efficiency at 300 keV were overestimated by about 6%, this would in turn introduce a 6% depression in the computed yield and intensity at this photon energy, which is about what is observed. It is planned to check the efficiency at 279 keV, with a calibrated ^{203}Hg source which is now on order.

(5) Finally, the intensity appears to fall off at very low photon energies - below about 100 keV. This effect appears to be real, and is probably a result of self-absorption in the target. (This will reemphasize that the results presented here are the yields and intensities emerging from a target of the given thickness - which should be carefully distinguished from the bremsstrahlung produced in the target. No attempt has been made in this work to remove the effects of absorption within the target).

Future Work

Future work planned in this laboratory will include a continuation of the experimental measurements of the thin target bremsstrahlung cross sections for aluminum, iron, carbon, tin and gold, over the energy range 0.1 to 3.0 MeV. Bremsstrahlung yields from thick targets of these materials will also be measured. An attempt will be made to measure these cross sections at forward angles ($0 < 15°$). Concurrent with these experiments, measurements of electron scattering from targets of these materials of various thicknesses will be made.

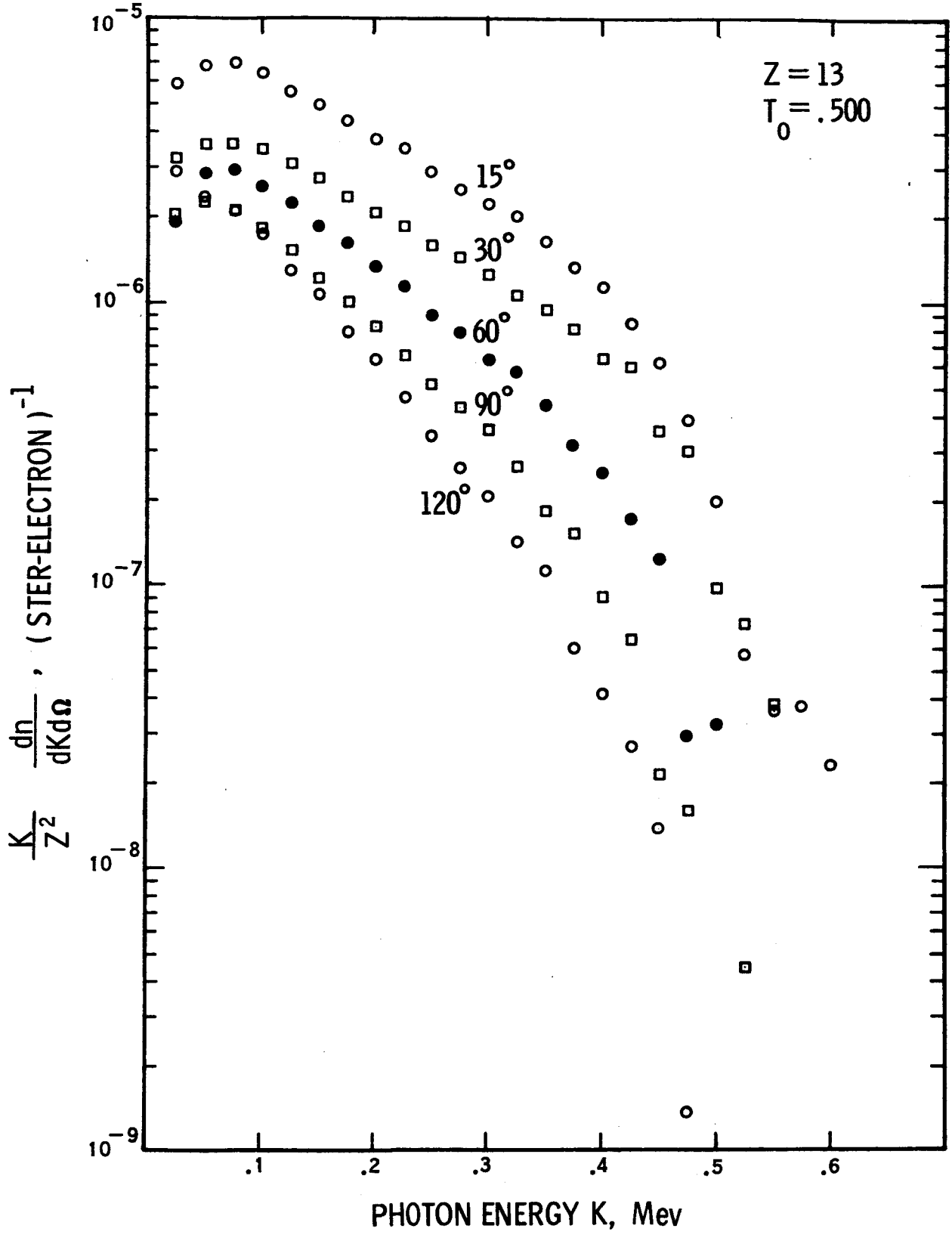

Figure 14. Reduced Intensity of Bremsstrahlung From a Thick Aluminum Target (0.5484 gm/cm^2) as a Function of Photon Energy

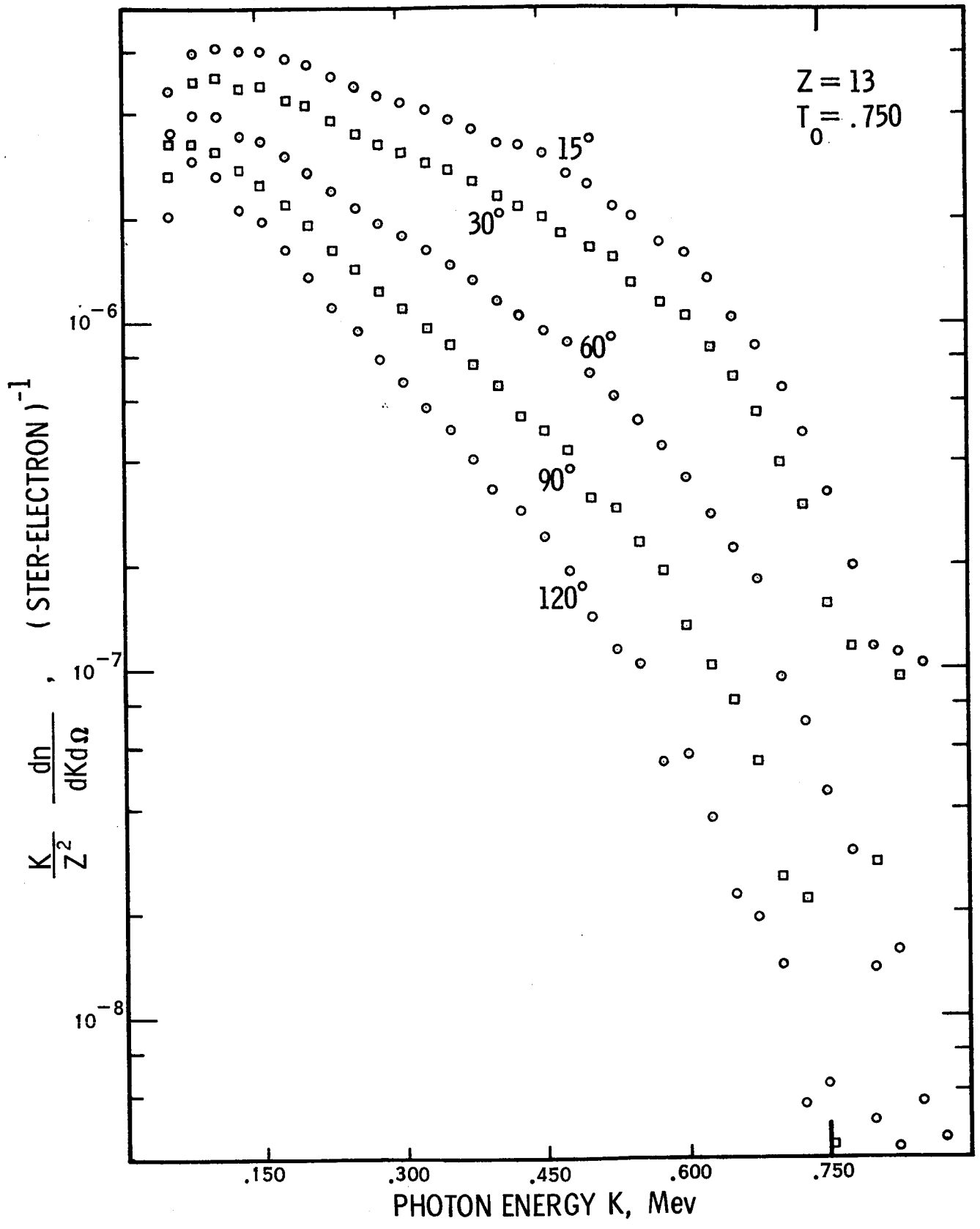

Figure 15. Reduced Intensity of Bremsstrahlung From a Thick Aluminum Target (0.5484 gm/cm^2) as a Function of Photon Energy

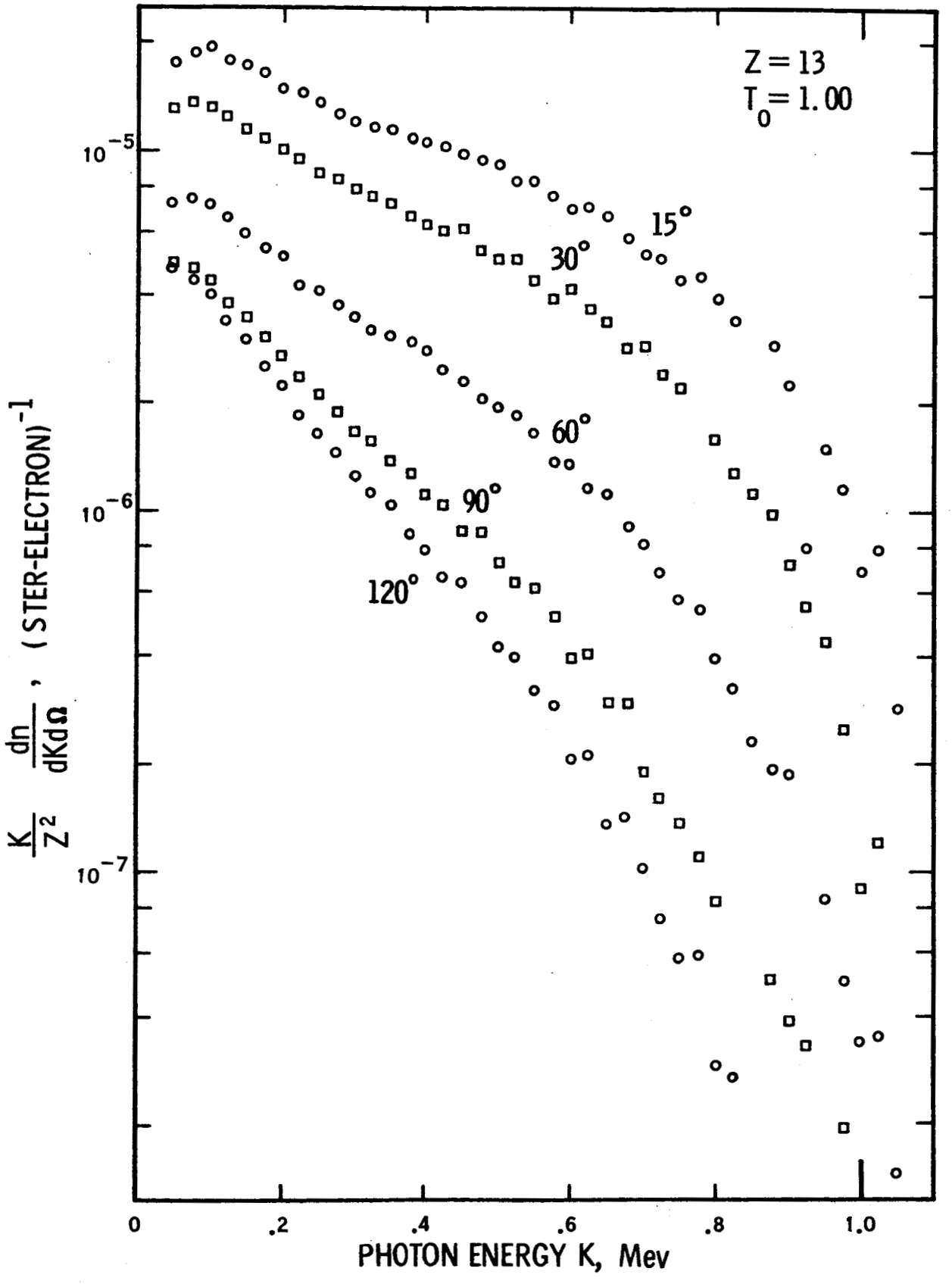

Figure 16. Reduced Intensity of Bremsstrahlung From a Thick Aluminum Target (0.5484 gm/cm^2) as a Function of Photon Energy

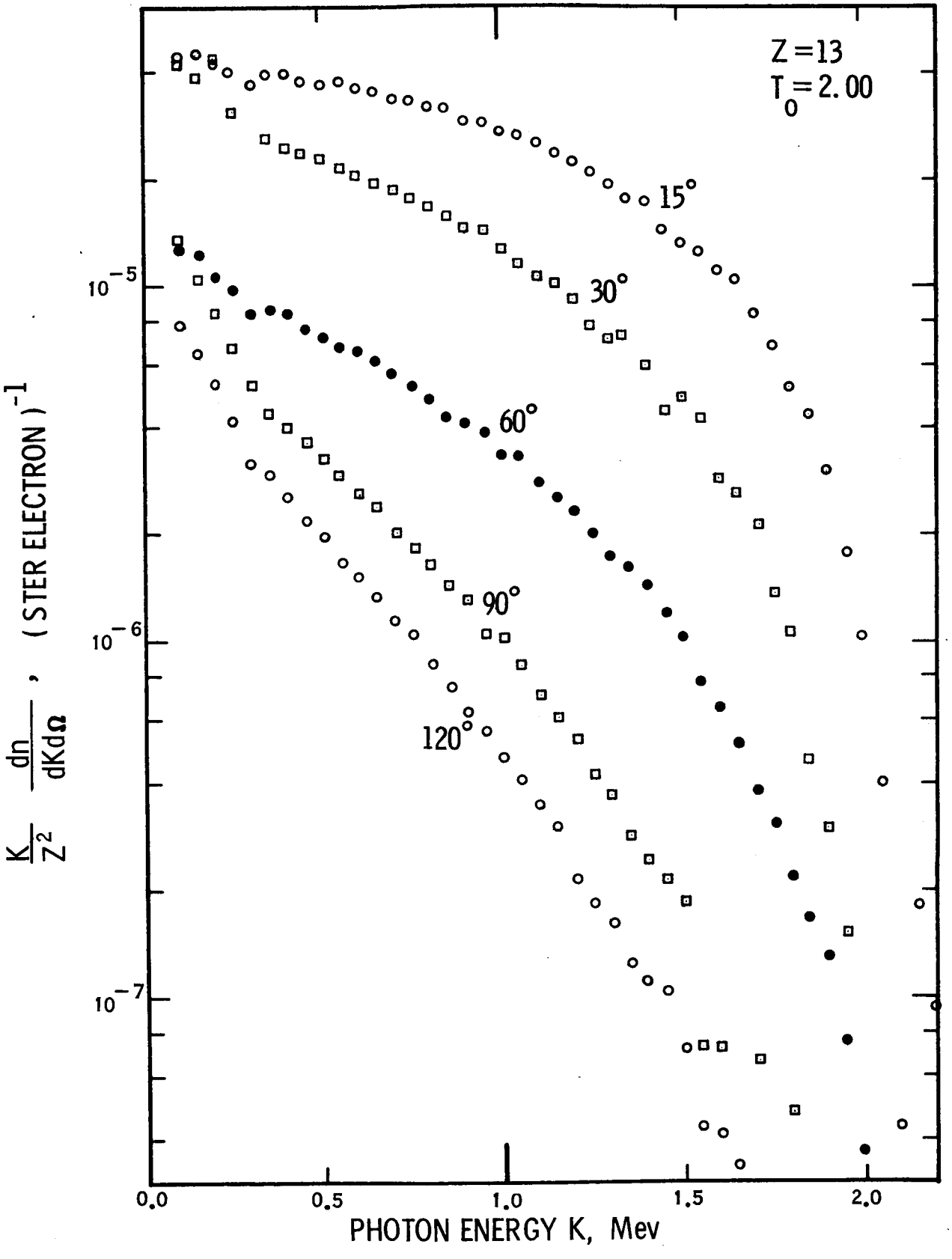

Figure 17. Reduced Intensity of Bremsstrahlung From a Thick Aluminum Target (1.878 gm/cm^2) as a Function of Photon Energy

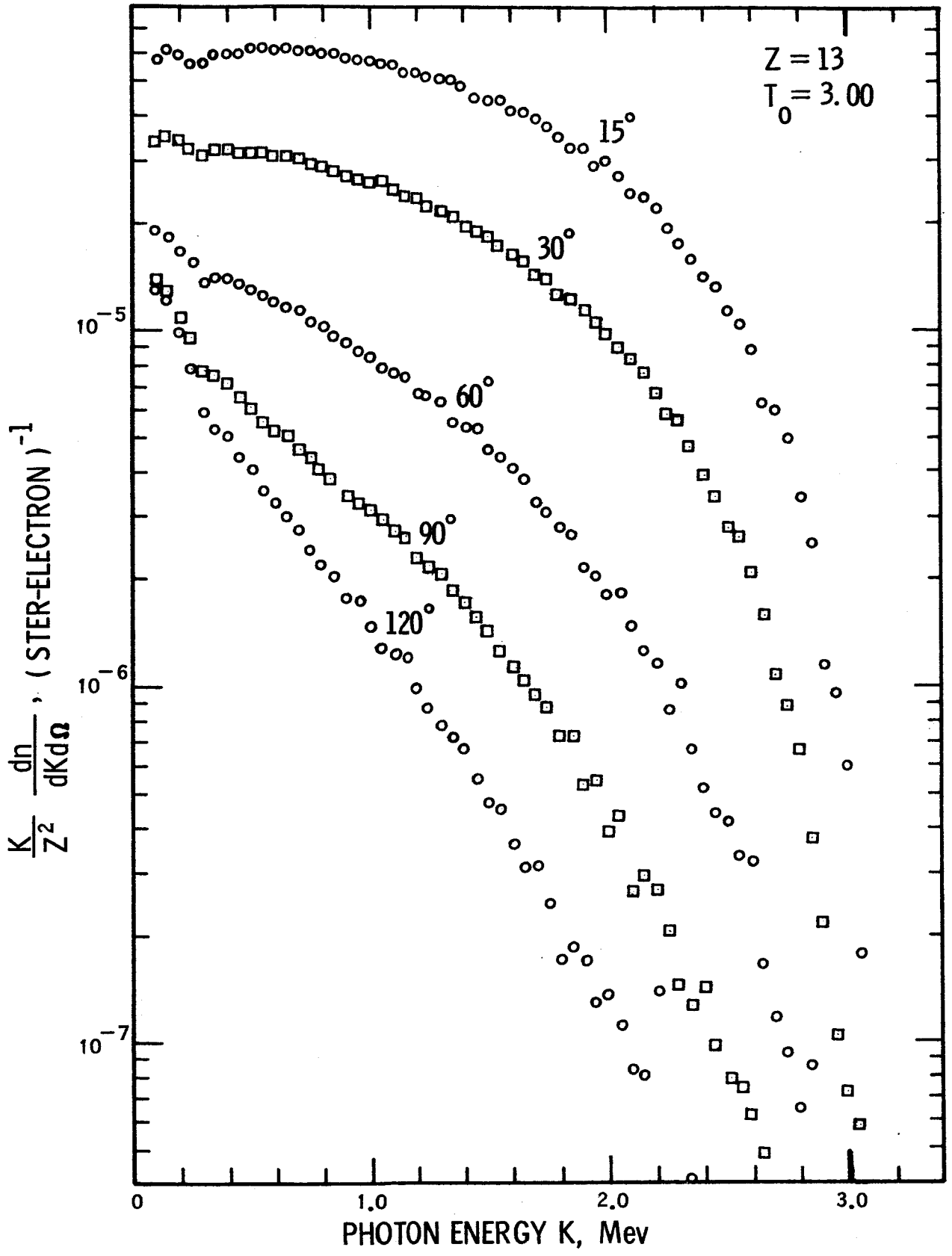

Figure 18. Reduced Intensity of Bremsstrahlung From a Thick Aluminum Target (1.878 gm/cm^2) as a Function of Photon Energy

TABLE 1

THICK TARGET BREMSSTRAHLUNG PRODUCTION

Material: ALUMINUM T_o 0.50

Thickness: 0.5484 GM/SQ CM θ 15.0

K Mev	$\frac{dn}{dK\ d\Omega}$ photon / Mev-ster-elect	$\frac{K}{Z^2}\frac{dn}{dK\ d\Omega}$ 1 / ster-electron	K Mev	$\frac{dn}{dK\ d\Omega}$ photon / Mev-ster-elect	$\frac{K}{Z^2}\frac{dn}{dK\ d\Omega}$ 1 / ster-electron
.025	.396 -1	.586 -5	.525	.186 -4	.579 -7
.050	.231 -1	.683 -5	.550	.112 -4	.366 -7
.075	.159 -1	.705 -5	.575	.111 -4	.378 -7
.100	.108 -1	.641 -5	.600	.650 -5	.231 -7
.125	.751 -2	.556 -5	.625		
.150	.557 -2	.495 -5	.650		
.175	.421 -2	.436 -5	.675		
.200	.320 -2	.379 -5	.700		
.225	.260 -2	.347 -5	.725		
.250	.195 -2	.289 -5	.750		
.275	.148 -2	.251 -5	.775		
.300	.126 -2	.223 -5	.800		
.325	.105 -2	.202 -5	.825		
.350	.790 -3	.164 -5	.850		
.375	.606 -3	.135 -5	.875		
.400	.489 -3	.116 -5	.900		
.425	.336 -3	.845 -6	.925		
.450	.228 -3	.607 -6	.950		
.475	.138 -3	.386 -6	.975		
.500	.675 -4	.200 -6	1.000		

TABLE 2

THICK TARGET BREMSSTRAHLUNG PRODUCTION

Material: ALUMINUM T_o 0.50

Thickness: 0.5484 GM/SQ CM θ 30.0

K Mev	$\frac{dn}{dK\ d\Omega}$ $\frac{\text{photon}}{\text{Mev-ster-elect}}$	$\frac{K}{Z^2}\frac{dn}{dK\ d\Omega}$ $\frac{1}{\text{ster-electron}}$	K Mev	$\frac{dn}{dK\ d\Omega}$ $\frac{\text{photon}}{\text{Mev-ster-elect}}$	$\frac{K}{Z^2}\frac{dn}{dK\ d\Omega}$ $\frac{1}{\text{ster-electron}}$
.025	.218 -1	.322 -5	.525	.239 -4	.744 -7
.050	.122 -1	.360 -5	.550	.117 -4	.381 -7
.075	.810 -2	.359 -5	.575	-.267 -6	-.703 -9
.100	.589 -2	.348 -5	.600	-.125 -6	-.443 -9
.125	.416 -2	.308 -5	.625		
.150	.308 -2	.273 -5	.650		
.175	.226 -2	.234 -5	.675		
.200	.175 -2	.207 -5	.700		
.225	.139 -2	.186 -5	.725		
.250	.108 -2	.160 -5	.750		
.275	.894 -3	.146 -5	.775		
.300	.722 -3	.128 -5	.800		
.325	.551 -3	.106 -5	.825		
.350	.463 -3	.958 -6	.850		
.375	.361 -3	.802 -6	.875		
.400	.270 -3	.638 -6	.900		
.425	.235 -3	.591 -6	.925		
.450.	.134 -3	.357 -6	.950		
.475	.108 -3	.304 -6	.975		
.500	.338 -4	.999 -7	1.000		

TABLE 3

THICK TARGET BREMSSTRAHLUNG PRODUCTION

Material: ALUMINUM T_o 0.50

Thickness: 0.5484 GM/SQ CM θ 60.0

K Mev	$\frac{dn}{dK\ d\Omega}$ $\frac{\text{photon}}{\text{Mev-ster-elect}}$	$\frac{K}{Z^2}\frac{dn}{dK\ d\Omega}$ $\frac{1}{\text{ster-electron}}$	K Mev	$\frac{dn}{dK\ d\Omega}$ $\frac{\text{photon}}{\text{Mev-ster-elect}}$	$\frac{K}{Z^2}\frac{dn}{dK\ d\Omega}$ $\frac{1}{\text{ster-electron}}$
.025	.130 -1	.193 -5	.525	-.638 -5	-.198 -7
.050	.970 -2	.287 -5	.550	.403 -6	.131 -8
.075	.660 -2	.293 -5	.575	-.287 -6	-.976 -9
.100	.433 -2	.256 -5	.600	.348 -5	.124 -7
.125	.298 -2	.221 -5	.625		
.150	.211 -2	.187 -5	.650		
.175	.156 -2	.161 -5	.675		
.200	.112 -2	.133 -5	.700		
.225	.858 -3	.114 -5	.725		
.250	.617 -3	.912 -6	.750		
.275	.491 -3	.798 -6	.775		
.300	.355 -3	.629 -6	.800		
.325	.300 -3	.578 -6	.825		
.350	.212 -3	.439 -6	.850		
.375	.141 -3	.313 -6	.875		
.400	.107 -3	.254 -6	.900		
.425	.686 -4	.173 -6	.925		
.450.	.477 -4	.127 -6	.950		
.475	.106 -4	.298 -7	.975		
.500	.111 -4	.328 -7	1.000		

TABLE 4

THICK TARGET BREMSSTRAHLUNG PRODUCTION

Material: ALUMINUM T_o 0.50

Thickness: 0.5484 GM/SQ CM θ 90.0

K Mev	$\frac{dn}{dK\, d\Omega}$ photon / Mev-ster-elect	$\frac{K}{Z^2}\frac{dn}{dK\, d\Omega}$ 1 / ster-electron	K Mev	$\frac{dn}{dK\, d\Omega}$ photon / Mev-ster-elect	$\frac{K}{Z^2}\frac{dn}{dK\, d\Omega}$ 1 / ster-electron
.025	.138 -1	.204 -5	.525	.145 -5	.451 -8
.050	.760 -2	.225 -5	.550	-.245 -6	-.798 -9
.075	.478 -2	.212 -5	.575	.924 -6	.314 -8
.100	.310 -2	.184 -5	.600	.319 -5	.113 -7
.125	.206 -2	.152 -5	.625		
.150	.139 -2	.123 -5	.650		
.175	.965 -3	.100 -5	.675		
.200	.691 -3	.818 -6	.700		
.225	.491 -3	.654 -6	.725		
.250	.344 -3	.509 -6	.750		
.275	.263 -3	.428 -6	.775		
.300	.200 -3	.354 -6	.800		
.325	.139 -3	.267 -6	.825		
.350	.888 -4	.184 -6	.850		
.375	.695 -4	.154 -6	.875		
.400	.389 -4	.920 -7	.900		
.425	.258 -4	.650 -7	.925		
.450.	.816 -5	.217 -7	.950		
.475	.572 -5	.161 -7	.975		
.500	.148 -6	.439 -9	1.000		

TABLE 5

THICK TARGET BREMSSTRAHLUNG PRODUCTION

Material: ALUMINUM T_o 0.50

Thickness: 0.5484 GM/SQ CM θ 120.0

K Mev	$\frac{dn}{dK\ d\Omega}$ photon / Mev-ster-elect	$\frac{K}{Z^2}\frac{dn}{dK\ d\Omega}$ 1 / ster-electron	K Mev	$\frac{dn}{dK\ d\Omega}$ photon / Mev-ster-elect	$\frac{K}{Z^2}\frac{dn}{dK\ d\Omega}$ 1 / ster-electron
.025	.198 -1	.293 -5	.525	.147 -6	.455 -9
.050	.804 -2	.238 -5	.550	-.141 -6	-.460 -9
.075	.479 -2	.213 -5	.575	.536 -5	.182 -7
.100	.291 -2	.172 -5	.600	-.468 -6	-.166 -8
.125	.174 -2	.129 -5	.625		
.150	.120 -2	.107 -5	.650		
.175	.758 -3	.785 -6	.675		
.200	.532 -3	.629 -6	.700		
.225	.346 -3	.461 -6	.725		
.250	.226 -3	.335 -6	.750		
.275	.160 -3	.260 -6	.775		
.300	.116 -3	.206 -6	.800		
.325	.742 -4	.143 -6	.825		
.350	.547 -4	.113 -6	.850		
.375	.272 -4	.604 -7	.875		
.400	.176 -4	.417 -7	.900		
.425	.108 -4	.271 -7	.925		
.450	.523 -5	.139 -7	.950		
.475	.495 -6	.139 -8	.975		
.500	-.602 -6	-.178 -8	1.000		

TABLE 6

THICK TARGET BREMSSTRAHLUNG PRODUCTION

Material: ALUMINUM T_o 0.75

Thickness: 0.5484 GM/SQ CM θ 15.0

K Mev	$\frac{dn}{dK\ d\Omega}$ $\frac{\text{photon}}{\text{Mev-ster-elect}}$	$\frac{K}{Z^2}\frac{dn}{dK\ d\Omega}$ $\frac{1}{\text{ster-electron}}$	K Mev	$\frac{dn}{dK\ d\Omega}$ $\frac{\text{photon}}{\text{Mev-ster-elect}}$	$\frac{K}{Z^2}\frac{dn}{dK\ d\Omega}$ $\frac{1}{\text{ster-electron}}$
.025			.525	.704 -3	.219 -5
.050	.156 -1	.461 -5	.550	.613 -3	.200 -5
.075	.134 -1	.594 -5	.575	.501 -3	.170 -5
.100	.104 -1	.614 -5	.600	.448 -3	.159 -5
.125	.815 -2	.603 -5	.625	.358 -3	.132 -5
.150	.678 -2	.601 -5	.650	.270 -3	.104 -5
.175	.555 -2	.575 -5	.675	.216 -3	.865 -6
.200	.462 -2	.547 -5	.700	.157 -3	.650 -6
.225	.381 -2	.508 -5	.725	.112 -3	.482 -6
.250	.322 -2	.476 -5	.750	.731 -4	.324 -6
.275	.278 -2	.453 -5	.775	.443 -4	.203 -6
.300	.243 -2	.432 -5	.800	.250 -4	.118 -6
.325	.213 -2	.410 -5	.825	.236 -4	.115 -6
.350	.184 -2	.379 -5	.850	.210 -4	.106 -6
.375	.161 -2	.357 -5	.875		
.400	.137 -2	.325 -5	.900		
.425	.127 -2	.320 -5	.925		
.450	.114 -2	.304 -5	.950		
.475	.946 -3	.266 -5	.975		
.500	.842 -3	.249 -5	1.000		

TABLE 7

THICK TARGET BREMSSTRAHLUNG PRODUCTION

Material: ALUMINUM T_o 0.75

Thickness: 0.5484 GM/SQ CM θ 30.0

K Mev	$\frac{dn}{dK\ d\Omega}$ photon / Mev-ster-elect	$\frac{K}{Z^2}\frac{dn}{dK\ d\Omega}$ 1 / ster-electron	K Mev	$\frac{dn}{dK\ d\Omega}$ photon / Mev-ster-elect	$\frac{K}{Z^2}\frac{dn}{dK\ d\Omega}$ 1 / ster-electron
.025			.525	.501 -3	.156 -5
.050	.112 -1	.331 -5	.550	.400 -3	.130 -5
.075	.112 -1	.496 -5	.575	.337 -3	.115 -5
.100	.864 -2	.511 -5	.600	.294 -3	.104 -5
.125	.638 -2	.472 -5	.625	.230 -3	.849 -6
.150	.540 -2	.479 -5	.650	.180 -3	.694 -6
.175	.421 -2	.436 -5	.675	.140 -3	.558 -6
.200	.353 -2	.418 -5	.700	.952 -4	.394 -6
.225	.287 -2	.382 -5	.725	.670 -4	.296 -6
.250	.235 -2	.347 -5	.750	.350 -4	.155 -6
.275	.200 -2	.325 -5	.775	.261 -4	.120 -6
.300	.175 -2	.310 -5	.800	.598 -5	.283 -7
.325	.150 -2	.288 -5	.825	.193 -4	.941 -7
.350	.132 -2	.273 -5	.850	.823 -5	.414 -7
.375	.114 -2	.253 -5	.875		
.400	.969 -3	.229 -5	.900		
.425	.852 -3	.214 -5	.925		
.450	.752 -3	.200 -5	.950		
.475	.639 -3	.180 -5	.975		
.500	.555 -3	.164 -5	1.000		

TABLE 8

THICK TARGET BREMSSTRAHLUNG PRODUCTION

Material: ALUMINUM T_o 0.75

Thickness: 0.5484 GM/SQ CM θ 60.0

K Mev	$\frac{dn}{dK\ d\Omega}$ photon / Mev-ster-elect	$\frac{K}{Z^2}\frac{dn}{dK\ d\Omega}$ 1 / ster-electron	K Mev	$\frac{dn}{dK\ d\Omega}$ photon / Mev-ster-elect	$\frac{K}{Z^2}\frac{dn}{dK\ d\Omega}$ 1 / ster-electron
.025			.525	.199 -3	.619 -6
.050	.120 -1	.354 -5	.550	.164 -3	.534 -6
.075	.896 -2	.398 -5	.575	.130 -3	.443 -6
.100	.661 -2	.391 -5	.600	.101 -3	.358 -6
.125	.463 -2	.342 -5	.625	.774 -4	.286 -6
.150	.375 -2	.333 -5	.650	.590 -4	.227 -6
.175	.290 -2	.301 -5	.675	.456 -4	.182 -6
.200	.229 -2	.271 -5	.700	.233 -4	.966 -7
.225	.181 -2	.241 -5	.725	.166 -4	.711 -7
.250	.146 -2	.216 -5	.750	.102 -4	.451 -7
.275	.118 -2	.192 -5	.775	.663 -5	.304 -7
.300	.101 -2	.179 -5	.800	.299 -5	.141 -7
.325	.840 -3	.162 -5	.825	.326 -5	.159 -7
.350	.708 -3	.147 -5	.850	.151 -5	.758 -8
.375	.594 -3	.132 -5	.875		
.400	.496 -3	.117 -5	.900		
.425	.418 -3	.105 -5	.925		
.450	.357 -3	.951 -6	.950		
.475	.310 -3	.872 -6	.975		
.500	.240 -3	.710 -6	1.000		

TABLE 9

THICK TARGET BREMSSTRAHLUNG PRODUCTION

Material: ALUMINUM T_o 0.75

Thickness: 0.5484 GM/SQ CM θ 90.0

K Mev	$\frac{dn}{dK\ d\Omega}$ photon / Mev-ster-elect	$\frac{K}{Z^2}\frac{dn}{dK\ d\Omega}$ 1 / ster-electron	K Mev	$\frac{dn}{dK\ d\Omega}$ photon / Mev-ster-elect	$\frac{K}{Z^2}\frac{dn}{dK\ d\Omega}$ 1 / ster-electron
.025			.525	.955 -4	.297 -6
.050	.890 -2	.263 -5	.550	.716 -4	.233 -6
.075	.743 -2	.330 -5	.575	.572 -4	.194 -6
.100	.528 -2	.313 -5	.600	.379 -4	.135 -6
.125	.374 -2	.277 -5	.625	.279 -4	.103 -6
.150	.283 -2	.251 -5	.650	.212 -4	.816 -7
.175	.209 -2	.217 -5	.675	.136 -4	.544 -7
.200	.163 -2	.193 -5	.700	.617 -5	.256 -7
.225	.122 -2	.162 -5	.725	.516 -5	.221 -7
.250	.963 -3	.142 -5	.750	.965 -6	.428 -8
.275	.757 -3	.123 -5	.775	.753 -6	.345 -8
.300	.620 -3	.110 -5	.800	.167 -5	.790 -8
.325	.501 -3	.963 -6	.825	.155 -5	.755 -8
.350	.412 -3	.852 -6	.850	.109 -5	.547 -8
.375	.339 -3	.752 -6	.875		
.400	.277 -3	.656 -6	.900		
.425	.215 -3	.541 -6	.925		
.450	.182 -3	.485 -6	.950		
.475	.153 -3	.431 -6	.975		
.500	.106 -3	.313 -6	1.000		

TABLE 10

THICK TARGET BREMSSTRAHLUNG PRODUCTION

Material: ALUMINUM T_o 0.75

Thickness: 0.5484 GM/SQ CM θ 120.0

K Mev	$\frac{dn}{dK\,d\Omega}$ $\frac{\text{photon}}{\text{Mev-ster-elect}}$	$\frac{K}{Z^2}\frac{dn}{dK\,d\Omega}$ $\frac{1}{\text{ster-electron}}$	K Mev	$\frac{dn}{dK\,d\Omega}$ $\frac{\text{photon}}{\text{Mev-ster-elect}}$	$\frac{K}{Z^2}\frac{dn}{dK\,d\Omega}$ $\frac{1}{\text{ster-electron}}$
.025			.525	.370 -4	.115 -6
.050	.684 -2	.202 -5	.550	.312 -4	.102 -6
.075	.656 -2	.291 -5	.575	.180 -4	.613 -7
.100	.448 -2	.265 -5	.600	.127 -4	.452 -7
.125	.288 -2	.213 -5	.625	.106 -4	.392 -7
.150	.221 -2	.196 -5	.650	.600 -5	.231 -7
.175	.155 -2	.161 -5	.675	.491 -5	.197 -7
.200	.114 -2	.135 -5	.700	.343 -5	.142 -7
.225	.834 -3	.111 -5	.725	.132 -5	.568 -8
.250	.644 -3	.953 -6	.750	.145 -5	.645 -8
.275	.480 -3	.780 -6	.775	-.473 -6	-.217 -8
.300	.385 -3	.684 -6	.800	.107 -5	.508 -8
.325	.296 -3	.569 -6	.825	.876 -6	.427 -8
.350	.239 -3	.495 -6	.850	.114 -5	.576 -8
.375	.182 -3	.404 -6	.875		
.400	.140 -3	.332 -6	.900		
.425	.115 -3	.290 -6	.925		
.450	.912 -4	.243 -6	.950		
.475	.683 -4	.192 -6	.975		
.500	.480 -4	.142 -6	1.000		

TABLE 11

THICK TARGET BREMSSTRAHLUNG PRODUCTION

Material: ALUMINUM T_o 1.00

Thickness: 0.5484 GM/SQ CM θ 15.0

K Mev	$\frac{dn}{dK\ d\Omega}$ photon / Mev-ster-elect	$\frac{K}{Z^2}\frac{dn}{dK\ d\Omega}$ 1 / ster-electron	K Mev	$\frac{dn}{dK\ d\Omega}$ photon / Mev-ster-elect	$\frac{K}{Z^2}\frac{dn}{dK\ d\Omega}$ 1 / ster-electron
.025			.525	.270 -2	.839 -5
.050	.601 -1	.178 -4	.550	.255 -2	.831 -5
.075	.428 -1	.190 -4	.575	.222 -2	.755 -5
.100	.322 -1	.190 -4	.600	.196 -2	.697 -5
.125	.242 -1	.179 -4	.625	.191 -2	.705 -5
.150	.193 -1	.171 -4	.650	.172 -2	.663 -5
.175	.157 -1	.162 -4	.675	.145 -2	.579 -5
.200	.125 -1	.150 -4	.700	.126 -2	.521 -5
.225	.108 -1	.144 -4	.725	.117 -2	.504 -5
.250	.918 -2	.136 -4	.750	.101 -2	.448 -5
.275	.783 -2	.127 -4	.775	.989 -3	.454 -5
.300	.676 -2	.120 -4	.800	.831 -3	.393 -5
.325	.615 -2	.118 -4	.825	.701 -3	.342 -5
.350	.557 -2	.115 -4	.850	.571 -3	.287 -5
.375	.491 -2	.109 -4	.875	.564 -3	.292 -5
.400	.450 -2	.106 -4	.900	.420 -3	.224 -5
.425	.408 -2	.102 -4	.925	.147 -3	.804 -6
.450	.375 -2	.998 -5	.950	.268 -3	.151 -5
.475	.340 -2	.956 -5	.975	.203 -3	.117 -5
.500	.307 -2	.907 -5	1.000	.116 -3	.686 -6
			1.025	.130 -3	.790 -6
			1.050	.460 -4	.286 -6
			1.075	.253 -4	.161 -6
			1.100	.188 -4	.122 -6

TABLE 12

THICK TARGET BREMSSTRAHLUNG PRODUCTION

Material: ALUMINUM T_o 1.00

Thickness: 0.5484 GM/SQ CM θ 30.0

K Mev	$\frac{dn}{dK\ d\Omega}$ photon / Mev-ster-elect	$\frac{K}{Z^2}\frac{dn}{dK\ d\Omega}$ 1 / ster-electron	K Mev	$\frac{dn}{dK\ d\Omega}$ photon / Mev-ster-elect	$\frac{K}{Z^2}\frac{dn}{dK\ d\Omega}$ 1 / ster-electron
.025			.525	.161 -2	.500 -5
.050	.444 -1	.131 -4	.550	.136 -2	.443 -5
.075	.308 -1	.137 -4	.575	.116 -2	.394 -5
.100	.225 -1	.133 -4	.600	.117 -2	.416 -5
.125	.170 -1	.127 -4	.625	.981 -3	.363 -5
.150	.132 -1	.117 -4	.650	.878 -3	.338 -5
.175	.106 -1	.109 -4	.675	.719 -3	.287 -5
.200	.858 -2	.102 -4	.700	.694 -3	.287 -5
.225	.713 -2	.950 -5	.725	.559 -3	.240 -5
.250	.591 -2	.874 -5	.750	.497 -3	.220 -5
.275	.514 -2	.837 -5	.775	.394 -3	.181 -5
.300	.440 -2	.782 -5	.800	.336 -3	.159 -5
.325	.390 -2	.751 -5	.825	.260 -3	.127 -5
.350	.344 -2	.712 -5	.850	.222 -3	.111 -5
.375	.300 -2	.665 -5	.875	.191 -3	.991 -6
.400	.269 -2	.638 -5	.900	.133 -3	.710 -6
.425	.239 -2	.602 -5	.925	.996 -4	.545 -6
.450	.226 -2	.603 -5	.950	.780 -4	.438 -6
.475	.190 -2	.535 -5	.975	.440 -4	.254 -6
.500	.170 -2	.502 -5	1.000	.152 -4	.901 -7
			1.025	.199 -4	.121 -6
			1.050	.246 -5	.153 -7
			1.075	.290 -5	.185 -7
			1.100	-.788 -6	-.513 -8

TABLE 13

THICK TARGET BREMSSTRAHLUNG PRODUCTION

Material: ALUMINUM T_o 1.00

Thickness: 0.5484 GM/SQ CM θ 60.0

K Mev	$\frac{dn}{dK\ d\Omega}$ photon / Mev-ster-elect	$\frac{K}{Z^2}\frac{dn}{dK\ d\Omega}$ 1 / ster-electron	K Mev	$\frac{dn}{dK\ d\Omega}$ photon / Mev-ster-elect	$\frac{K}{Z^2}\frac{dn}{dK\ d\Omega}$ 1 / ster-electron
.025			.525	.597 -3	.185 -5
.050	.245 -1	.724 -5	.550	.516 -3	.168 -5
.075	.168 -1	.748 -5	.575	.410 -3	.140 -5
.100	.122 -1	.721 -5	.600	.381 -3	.135 -5
.125	.877 -2	.648 -5	.625	.320 -3	.118 -5
.150	.674 -2	.598 -5	.650	.293 -3	.113 -5
.175	.521 -2	.539 -5	.675	.230 -3	.918 -6
.200	.429 -2	.508 -5	.700	.197 -3	.815 -6
.225	.336 -2	.448 -5	.725	.159 -3	.683 -6
.250	.282 -2	.418 -5	.750	.129 -3	.574 -6
.275	.231 -2	.376 -5	.775	.118 -3	.542 -6
.300	.196 -2	.348 -5	.800	.832 -4	.394 -6
.325	.174 -2	.335 -5	.825	.662 -4	.323 -6
.350	.149 -2	.309 -5	.850	.453 -4	.303 -6
.375	.134 -2	.296 -5	.875	.369 -4	.191 -6
.400	.117 -2	.277 -5	.900	.352 -4	.188 -6
.425	.988 -3	.248 -5	.925	.302 -4	.165 -6
.450.	.856 -3	.228 -5	.950	.149 -4	.840 -7
.475	.749 -3	.211 -5	.975	.867 -5	.500 -7
.500	.662 -3	.196 -5	1.000	.580 -5	.343 -7
			1.025	.580 -5	.352 -7
			1.050	.234 -5	.146 -7
			1.075	.165 -5	.105 -7
			1.100	.142 -5	.924 -8

TABLE 14

THICK TARGET BREMSSTRAHLUNG PRODUCTION

Material: ALUMINUM T_o 1.00

Thickness: 0.5484 GM/SQ CM θ 90.0

K Mev	$\frac{dn}{dK\ d\Omega}$ photon / Mev-ster-elect	$\frac{K}{Z^2}\frac{dn}{dK\ d\Omega}$ 1 / ster-electron	K Mev	$\frac{dn}{dK\ d\Omega}$ photon / Mev-ster-elect	$\frac{K}{Z^2}\frac{dn}{dK\ d\Omega}$ 1 / ster-electron
.025			.525	.208 -3	.645 -6
.050	.169 -1	.499 -5	.550	.190 -3	.620 -6
.075	.107 -1	.476 -5	.575	.149 -3	.508 -6
.100	.751 -2	.444 -5	.600	.111 -3	.393 -6
.125	.519 -2	.384 -5	.625	.110 -3	.406 -6
.150	.392 -2	.348 -5	.650	.780 -4	.300 -6
.175	.292 -2	.302 -5	.675	.750 -4	.299 -6
.200	.228 -2	.270 -5	.700	.603 -4	.250 -6
.225	.175 -2	.233 -5	.725	.450 -4	.193 -6
.250	.143 -2	.211 -5	.750	.364 -4	.162 -6
.275	.116 -2	.189 -5	.775	.301 -4	.138 -6
.300	.932 -3	.165 -5	.800	.235 -4	.111 -6
.325	.820 -3	.158 -5	.825	.172 -4	.840 -7
.350	.669 -3	.139 -5	.850	.107 -4	.537 -7
.375	.578 -3	.128 -5	.875	.975 -5	.505 -7
.400	.473 -3	.112 -5	.900	.724 -5	.386 -7
.425	.416 -3	.105 -5	.925	.606 -5	.332 -7
.450	.333 -3	.887 -6	.950	.146 -5	.822 -8
.475	.314 -3	.884 -6	.975	.342 -5	.197 -7
.500	.247 -3	.732 -6	1.000	-.208 -5	-.123 -7
			1.025	.182 -5	.110 -7
			1.050	-.538 -6	-.334 -8
			1.075	.165 -5	.105 -7
			1.100	.833 -7	.542 -9

TABLE 15

THICK TARGET BREMSSTRAHLUNG PRODUCTION

Material: ALUMINUM T_o 1.00

Thickness: 0.5484 GM/SQ CM θ 120.0

K Mev	$\frac{dn}{dK\ d\Omega}$ photon / Mev-ster-elect	$\frac{K}{Z^2}\frac{dn}{dK\ d\Omega}$ 1 / ster-electron	K Mev	$\frac{dn}{dK\ d\Omega}$ photon / Mev-ster-elect	$\frac{K}{Z^2}\frac{dn}{dK\ d\Omega}$ 1 / ster-electron
.025			.525	.128 -3	.397 -6
.050	.162 -1	.478 -5	.550	.987 -4	.321 -6
.075	.998 -2	.443 -5	.575	.859 -4	.292 -6
.100	.681 -2	.403 -5	.600	.579 -4	.205 -6
.125	.459 -2	.340 -5	.625	.570 -4	.211 -6
.150	.341 -2	.303 -5	.650	.358 -4	.138 -6
.175	.245 -2	.254 -5	.675	.355 -4	.142 -6
.200	.189 -2	.224 -5	.700	.247 -4	.102 -6
.225	.139 -2	.185 -5	.725	.174 -4	.745 -7
.250	.111 -2	.164 -5	.750	.131 -4	.580 -7
.275	.889 -3	.145 -5	.775	.128 -4	.589 -7
.300	.710 -3	.126 -5	.800	.614 -5	.291 -7
.325	.587 -3	.113 -5	.825	.554 -5	.270 -7
.350	.502 -3	.104 -5	.850	.552 -5	.278 -7
.375	.394 -3	.875 -6	.875	.187 -5	.968 -8
.400	.333 -3	.788 -6	.900	.208 -5	.111 -7
.425	.262 -3	.660 -6	.925	.111 -5	.605 -8
.450	.241 -3	.642 -6	.950	-.199 -6	-.112 -8
.475	.182 -3	.512 -6	.975	-.481 -6	-.277 -8
.500	.144 -3	.426 -6	1.000	.189 -5	.112 -7
			1.025	-.116 -7	-.703 -10
			1.050	.161 -7	.999 -10
			1.075	.931 -7	.592 -9
			1.100	-.852 -7	-.555 -9

TABLE 16

THICK TARGET BREMSSTRAHLUNG PRODUCTION

Material: ALUMINUM T_o 2.00

Thickness: 1.878 GM/SQ CM θ 15.0

K Mev	$\frac{dn}{dK\,d\Omega}$ $\frac{\text{photon}}{\text{Mev-ster-elect}}$	$\frac{K}{Z^2}\frac{dn}{dK\,d\Omega}$ $\frac{1}{\text{ster-electron}}$	K Mev	$\frac{dn}{dK\,d\Omega}$ $\frac{\text{photon}}{\text{Mev-ster-elect}}$	$\frac{K}{Z^2}\frac{dn}{dK\,d\Omega}$ $\frac{1}{\text{ster-electron}}$
.05			1.55	.137 -2	.126 -4
.10	.738 -1	.437 -4	1.60	.116 -2	.110 -4
.15	.500 -1	.443 -4	1.65	.106 -2	.104 -4
.20	.354 -1	.418 -4	1.70	.834 -3	.839 -5
.25	.269 -1	.398 -4	1.75	.656 -3	.679 -5
.30	.207 -1	.368 -4	1.80	.481 -3	.512 -5
.35	.191 -1	.396 -4	1.85	.400 -3	.438 -5
.40	.166 -1	.393 -4	1.90	.269 -3	.302 -5
.45	.142 -1	.377 -4	1.95	.155 -3	.179 -5
.50	.125 -1	.370 -4	2.00	.865 -4	.102 -5
.55	.115 -1	.373 -4	2.05	.335 -4	.407 -6
.60	.102 -1	.364 -4	2.10	.353 -5	.439 -7
.65	.922 -2	.355 -4	2.15	.144 -4	.184 -6
.70	.817 -2	.338 -4	2.20	.721 -5	.938 -7
.75	.744 -2	.330 -4	2.25		
.80	.673 -2	.319 -4	2.30		
.85	.629 -2	.315 -4	2.35		
.90	.543 -2	.289 -4	2.40		
.95	.512 -2	.288 -4	2.45		
1.00	.453 -2	.268 -4	2.50		
1.05	.425 -2	.264 -4	2.55		
1.10	.382 -2	.249 -4	2.60		
1.15	.344 -2	.234 -4	2.65		
1.20	.319 -2	.227 -4	2.70		
1.25	.283 -2	.209 -4	2.75		
1.30	.250 -2	.192 -4	2.80		
1.35	.224 -2	.178 -4	2.85		
1.40	.207 -2	.172 -4	2.90		
1.45	.167 -2	.143 -4	2.95		
1.50	.150 -2	.133 -4	3.00		

TABLE 17

THICK TARGET BREMSSTRAHLUNG PRODUCTION

Material: ALUMINUM T_o 2.00

Thickness: 1.878 GM/SQ CM θ 30.0

K Mev	$\frac{dn}{dK\,d\Omega}$ photon / Mev-ster-elect	$\frac{K}{Z^2}\frac{dn}{dK\,d\Omega}$ 1 / ster-electron	K Mev	$\frac{dn}{dK\,d\Omega}$ photon / Mev-ster-elect	$\frac{K}{Z^2}\frac{dn}{dK\,d\Omega}$ 1 / ster-electron
.05			1.55	.462 -3	.424 -5
.10	.722 -1	.427 -4	1.60	.302 -3	.286 -5
.15	.425 -1	.386 -4	1.65	.266 -3	.260 -5
.20	.278 -1	.329 -4	1.70	.210 -3	.211 -5
.25	.206 -1	.304 -4	1.75	.132 -3	.137 -5
.30	.154 -1	.274 -4	1.80	.998 -4	.106 -5
.35	.125 -1	.258 -4	1.85	.421 -4	.461 -6
.40	.103 -1	.244 -4	1.90	.264 -4	.297 -6
.45	.886 -2	.236 -4	1.95	.130 -5	.151 -7
.50	.771 -2	.228 -4	2.00	-.125 -5	-.148 -7
.55	.660 -2	.215 -4	2.05	.723 -6	.877 -8
.60	.569 -2	.202 -4	2.10	.437 -5	.543 -7
.65	.504 -2	.194 -4	2.15	.135 -4	.172 -6
.70	.448 -2	.186 -4	2.20	-.318 -5	-.414 -7
.75	.397 -2	.176 -4	2.25		
.80	.345 -2	.163 -4	2.30		
.85	.309 -2	.155 -4	2.35		
.90	.267 -2	.142 -4	2.40		
.95	.251 -2	.141 -4	2.45		
1.00	.214 -2	.127 -4	2.50		
1.05	.183 -2	.114 -4	2.55		
1.10	.167 -2	.108 -4	2.60		
1.15	.149 -2	.101 -4	2.65		
1.20	.127 -2	.900 -5	2.70		
1.25	.104 -2	.767 -5	2.75		
1.30	.921 -3	.709 -5	2.80		
1.35	.902 -3	.720 -5	2.85		
1.40	.714 -3	.592 -5	2.90		
1.45	.519 -3	.445 -5	2.95		
1.50	.545 -3	.483 -5	3.00		

TABLE 18

THICK TARGET BREMSSTRAHLUNG PRODUCTION

Material: ALUMINUM T_o 2.00

Thickness: 1.878 GM/SQ CM θ 60.0

K Mev	$\frac{dn}{dK\,d\Omega}$ photon / Mev-ster-elect	$\frac{K}{Z^2}\frac{dn}{dK\,d\Omega}$ 1 / ster-electron	K Mev	$\frac{dn}{dK\,d\Omega}$ photon / Mev-ster-elect	$\frac{K}{Z^2}\frac{dn}{dK\,d\Omega}$ 1 / ster-electron
.05			1.55	.848 -4	.778 -6
.10	.216 -1	.128 -4	1.60	.683 -4	.647 -6
.15	.137 -1	.121 -4	1.65	.535 -4	.522 -6
.20	.907 -2	.107 -4	1.70	.382 -4	.384 -6
.25	.665 -2	.984 -5	1.75	.294 -4	.304 -6
.30	.474 -2	.841 -5	1.80	.207 -4	.221 -6
.35	.416 -2	.861 -5	1.85	.154 -4	.168 -6
.40	.350 -2	.828 -5	1.90	.115 -4	.130 -6
.45	.288 -2	.767 -5	1.95	.666 -5	.768 -7
.50	.249 -2	.737 -5	2.00	.318 -5	.376 -7
.55	.208 -2	.677 -5	2.05	.158 -5	.192 -7
.60	.183 -2	.648 -5	2.10	.151 -5	.188 -7
.65	.159 -2	.611 -5	2.15	.790 -6	.100 -7
.70	.138 -2	.572 -5	2.20	.863 -6	.112 -7
.75	.119 -2	.526 -5	2.25		
.80	.103 -2	.487 -5	2.30		
.85	.869 -3	.435 -5	2.35		
.90	.777 -3	.414 -5	2.40		
.95	.696 -3	.391 -5	2.45		
1.00	.569 -3	.336 -5	2.50		
1.05	.542 -3	.336 -5	2.55		
1.10	.438 -3	.285 -5	2.60		
1.15	.380 -3	.259 -5	2.65		
1.20	.328 -3	.233 -5	2.70		
1.25	.272 -3	.202 -5	2.75		
1.30	.231 -3	.178 -5	2.80		
1.35	.204 -3	.163 -5	2.85		
1.40	.173 -3	.143 -5	2.90		
1.45	.141 -3	.121 -5	2.95		
1.50	.115 -3	.102 -5	3.00		

TABLE 19

THICK TARGET BREMSSTRAHLUNG PRODUCTION

Material: ALUMINUM T_o 2.00

Thickness: 1.878 GM/SQ CM θ 90.0

K Mev	$\frac{dn}{dK\ d\Omega}$ $\frac{\text{photon}}{\text{Mev-ster-elect}}$	$\frac{K}{Z^2}\frac{dn}{dK\ d\Omega}$ $\frac{1}{\text{ster-electron}}$	K Mev	$\frac{dn}{dK\ d\Omega}$ $\frac{\text{photon}}{\text{Mev-ster-elect}}$	$\frac{K}{Z^2}\frac{dn}{dK\ d\Omega}$ $\frac{1}{\text{ster-electron}}$
.05			1.55	.802 -5	.735 -7
.10	.218 -1	.129 -4	1.60	.767 -5	.726 -7
.15	.117 -1	.104 -4	1.65	.140 -5	.137 -7
.20	.703 -2	.832 -5	1.70	.674 -5	.678 -7
.25	.446 -2	.660 -5	1.75	.284 -5	.294 -7
.30	.297 -2	.528 -5	1.80	.451 -5	.480 -7
.35	.225 -2	.466 -5	1.85	.139 -5	.152 -7
.40	.169 -2	.400 -5	1.90	.460 -6	.517 -8
.45	.136 -2	.362 -5	1.95	-.110 -6	-.126 -8
.50	.111 -2	.328 -5	2.00	.658 -6	.779 -8
.55	.902 -3	.293 -5	2.05	-.185 -6	-.225 -8
.60	.733 -3	.260 -5	2.10	.458 -6	.569 -8
.65	.628 -3	.241 -5	2.15	.125 -6	.159 -8
.70	.487 -3	.202 -5	2.20	.915 -6	.119 -7
.75	.408 -3	.181 -5	2.25		
.80	.352 -3	.166 -5	2.30		
.85	.285 -3	.143 -5	2.35		
.90	.245 -3	.131 -5	2.40		
.95	.187 -3	.105 -5	2.45		
1.00	.172 -3	.102 -5	2.50		
1.05	.138 -3	.858 -6	2.55		
1.10	.108 -3	.701 -6	2.60		
1.15	.908 -4	.617 -6	2.65		
1.20	.740 -4	.525 -6	2.70		
1.25	.569 -4	.420 -6	2.75		
1.30	.480 -4	.369 -6	2.80		
1.35	.353 -4	.282 -6	2.85		
1.40	.292 -4	.242 -6	2.90		
1.45	.252 -4	.216 -6	2.95		
1.50	.211 -4	.187 -6	3.00		

TABLE 20

THICK TARGET BREMSSTRAHLUNG PRODUCTION

Material: ALUMINUM T_o 2.00

Thickness: 1.878 GM/SQ CM θ 120.0

K Mev	$\frac{dn}{dK\,d\Omega}$ photon / Mev-ster-elect	$\frac{K}{Z^2}\frac{dn}{dK\,d\Omega}$ 1 / ster-electron	K Mev	$\frac{dn}{dK\,d\Omega}$ photon / Mev-ster-elect	$\frac{K}{Z^2}\frac{dn}{dK\,d\Omega}$ 1 / ster-electron
.05			1.55	.474 -5	.435 -7
.10	.130 -1	.769 -5	1.60	.435 -5	.412 -7
.15	.738 -2	.655 -5	1.65	.351 -5	.343 -7
.20	.449 -2	.532 -5	1.70	.206 -5	.207 -7
.25	.276 -2	.408 -5	1.75	.176 -5	.182 -7
.30	.177 -2	.314 -5	1.80	.933 -6	.994 -8
.35	.140 -2	.290 -5	1.85	.152 -5	.167 -7
.40	.108 -2	.256 -5	1.90	.673 -6	.756 -8
.45	.824 -3	.219 -5	1.95	.295 -6	.341 -8
.50	.656 -3	.194 -5	2.00	.480 -6	.568 -8
.55	.521 -3	.170 -5	2.05	.913 -7	.111 -8
.60	.430 -3	.153 -5	2.10	.951 -7	.118 -8
.65	.342 -3	.132 -5	2.15	.487 -7	.620 -9
.70	.278 -3	.115 -5	2.20	.354 -6	.461 -8
.75	.236 -3	.105 -5	2.25		
.80	.180 -3	.850 -6	2.30		
.85	.149 -3	.747 -6	2.35		
.90	.120 -3	.637 -6	2.40		
.95	.997 -4	.560 -6	2.45		
1.00	.797 -4	.472 -6	2.50		
1.05	.651 -4	.404 -6	2.55		
1.10	.537 -4	.350 -6	2.60		
1.15	.450 -4	.306 -6	2.65		
1.20	.304 -4	.216 -6	2.70		
1.25	.253 -4	.187 -6	2.75		
1.30	.212 -4	.163 -6	2.80		
1.35	.159 -4	.127 -6	2.85		
1.40	.127 -4	.105 -6	2.90		
1.45	.120 -4	.103 -6	2.95		
1.50	.793 -5	.704 -7	3.00		

TABLE 21

THICK TARGET BREMSSTRAHLUNG PRODUCTION

Material: ALUMINUM T_o 3.00

Thickness: 1.878 GM/SQ CM θ 15.0

K Mev	$\frac{dn}{dK\ d\Omega}$ photon / Mev-ster-elect	$\frac{K}{Z^2}\frac{dn}{dK\ d\Omega}$ 1 / ster-electron	K Mev	$\frac{dn}{dK\ d\Omega}$ photon / Mev-ster-elect	$\frac{K}{Z^2}\frac{dn}{dK\ d\Omega}$ 1 / ster-electron
.05			1.55	.483 -2	.443 -4
.10	.963 -1	.570 -4	1.60	.438 -2	.415 -4
.15	.682 -1	.605 -4	1.65	.417 -2	.407 -4
.20	.501 -1	.593 -4	1.70	.392 -2	.394 -4
.25	.377 -1	.558 -4	1.75	.361 -2	.374 -4
.30	.318 -1	.564 -4	1.80	.329 -2	.350 -4
.35	.289 -1	.598 -4	1.85	.297 -2	.325 -4
.40	.253 -1	.599 -4	1.90	.291 -2	.327 -4
.45	.225 -1	.600 -4	1.95	.253 -2	.292 -4
.50	.207 -1	.613 -4	2.00	.254 -2	.300 -4
.55	.190 -1	.619 -4	2.05	.225 -2	.273 -4
.60	.172 -1	.612 -4	2.10	.195 -2	.242 -4
.65	.161 -1	.618 -4	2.15	.188 -2	.239 -4
.70	.147 -1	.608 -4	2.20	.170 -2	.222 -4
.75	.137 -1	.608 -4	2.25	.146 -2	.194 -4
.80	.126 -1	.598 -4	2.30	.131 -2	.178 -4
.85	.118 -1	.595 -4	2.35	.115 -2	.160 -4
.90	.109 -1	.581 -4	2.40	.101 -2	.143 -4
.95	.102 -1	.574 -4	2.45	.917 -3	.133 -4
1.00	.967 -2	.572 -4	2.50	.770 -3	.114 -4
1.05	.901 -2	.560 -4	2.55	.689 -3	.104 -4
1.10	.854 -2	.556 -4	2.60	.575 -3	.884 -5
1.15	.777 -2	.529 -4	2.65	.401 -3	.628 -5
1.20	.744 -2	.528 -4	2.70	.374 -3	.598 -5
1.25	.688 -2	.509 -4	2.75	.307 -3	.500 -5
1.30	.658 -2	.506 -4	2.80	.206 -3	.342 -5
1.35	.627 -2	.501 -4	2.85	.152 -3	.257 -5
1.40	.587 -2	.486 -4	2.90	.676 -4	.116 -5
1.45	.524 -2	.450 -4	2.95	.553 -4	.966 -6
1.50	.499 -2	.443 -4	3.00	.337 -4	.599 -6

TABLE 22

THICK TARGET BREMSSTRAHLUNG PRODUCTION

Material: ALUMINUM T_o 3.00

Thickness: 1.878 GM/SQ CM θ 30.0

K Mev	$\frac{dn}{dK\,d\Omega}$ photon / Mev-ster-elect	$\frac{K}{Z^2}\frac{dn}{dK\,d\Omega}$ 1 / ster-electron	K Mev	$\frac{dn}{dK\,d\Omega}$ photon / Mev-ster-elect	$\frac{K}{Z^2}\frac{dn}{dK\,d\Omega}$ 1 / ster-electron
.05			1.55	.189 -2	.173 -4
.10	.573 -1	.339 -4	1.60	.175 -2	.165 -4
.15	.396 -1	.352 -4	1.65	.162 -2	.158 -4
.20	.290 -1	.343 -4	1.70	.144 -2	.145 -4
.25	.218 -1	.322 -4	1.75	.136 -2	.141 -4
.30	.175 -1	.311 -4	1.80	.120 -2	.128 -4
.35	.156 -1	.323 -4	1.85	.110 -2	.120 -4
.40	.136 -1	.323 -4	1.90	.101 -2	.113 -4
.45	.119 -1	.317 -4	1.95	.914 -3	.105 -4
.50	.107 -1	.317 -4	2.00	.831 -3	.983 -5
.55	.969 -2	.316 -4	2.05	.744 -3	.903 -5
.60	.878 -2	.312 -4	2.10	.682 -3	.848 -5
.65	.800 -2	.308 -4	2.15	.600 -3	.764 -5
.70	.729 -2	.302 -4	2.20	.517 -3	.673 -5
.75	.661 -2	.293 -4	2.25	.448 -3	.596 -5
.80	.612 -2	.290 -4	2.30	.423 -3	.575 -5
.85	.560 -2	.282 -4	2.35	.340 -3	.473 -5
.90	.515 -2	.274 -4	2.40	.279 -3	.396 -5
.95	.476 -2	.268 -4	2.45	.239 -3	.346 -5
1.00	.438 -2	.259 -4	2.50	.190 -3	.281 -5
1.05	.419 -2	.260 -4	2.55	.174 -3	.263 -5
1.10	.380 -2	.247 -4	2.60	.136 -3	.209 -5
1.15	.350 -2	.238 -4	2.65	.101 -3	.159 -5
1.20	.329 -2	.234 -4	2.70	.677 -4	.108 -5
1.25	.302 -2	.224 -4	2.75	.541 -4	.881 -6
1.30	.282 -2	.217 -4	2.80	.400 -4	.663 -6
1.35	.261 -2	.209 -4	2.85	.222 -4	.375 -6
1.40	.239 -2	.198 -4	2.90	.127 -4	.218 -6
1.45	.222 -2	.190 -4	2.95	.598 -5	.104 -6
1.50	.208 -2	.185 -4	3.00	.408 -5	.724 -7

TABLE 23

THICK TARGET BREMSSTRAHLUNG PRODUCTION

Material: ALUMINUM T_o 3.00

Thickness: 1.878 GM/SQ CM θ 60.0

K Mev	$\frac{dn}{dK\ d\Omega}$ photon / Mev-ster-elect	$\frac{K}{Z^2}\frac{dn}{dK\ d\Omega}$ 1 / ster-electron	K Mev	$\frac{dn}{dK\ d\Omega}$ photon / Mev-ster-elect	$\frac{K}{Z^2}\frac{dn}{dK\ d\Omega}$ 1 / ster-electron
.05			1.55	.483 -3	.444 -5
.10	.327 -1	.193 -4	1.60	.437 -3	.414 -5
.15	.209 -1	.185 -4	1.65	.393 -3	.384 -5
.20	.143 -1	.169 -4	1.70	.329 -3	.331 -5
.25	.106 -1	.156 -4	1.75	.301 -3	.311 -5
.30	.775 -2	.138 -4	1.80	.263 -3	.281 -5
.35	.685 -2	.142 -4	1.85	.245 -3	.268 -5
.40	.594 -2	.141 -4	1.90	.193 -3	.217 -5
.45	.508 -2	.135 -4	1.95	.177 -3	.205 -5
.50	.441 -2	.131 -4	2.00	.154 -3	.182 -5
.55	.384 -2	.125 -4	2.05	.151 -3	.183 -5
.60	.341 -2	.121 -4	2.10	.120 -3	.149 -5
.65	.307 -2	.118 -4	2.15	.998 -4	.127 -5
.70	.269 -2	.111 -4	2.20	.901 -4	.117 -5
.75	.238 -2	.106 -4	2.25	.651 -4	.867 -6
.80	.215 -2	.102 -4	2.30	.752 -4	.102 -5
.85	.193 -2	.967 -5	2.35	.481 -4	.668 -6
.90	.173 -2	.923 -5	2.40	.368 -4	.522 -6
.95	.158 -2	.889 -5	2.45	.310 -4	.450 -6
1.00	.143 -2	.843 -5	2.50	.287 -4	.424 -6
1.05	.129 -2	.794 -5	2.55	.223 -4	.336 -6
1.10	.116 -2	.757 -5	2.60	.212 -4	.326 -6
1.15	.109 -2	.744 -5	2.65	.105 -4	.165 -6
1.20	.952 -3	.676 -5	2.70	.741 -5	.118 -6
1.25	.886 -3	.658 -5	2.75	.575 -5	.936 -7
1.30	.821 -3	.631 -5	2.80	.392 -5	.649 -7
1.35	.688 -3	.549 -5	2.85	.515 -5	.868 -7
1.40	.648 -3	.537 -5	2.90	.232 -5	.397 -7
1.45	.618 -3	.530 -5	2.95	.174 -5	.305 -7
1.50	.524 -3	.465 -5	3.00	.981 -6	.174 -7

TABLE 24

THICK TARGET BREMSSTRAHLUNG PRODUCTION

Material: ALUMINUM T_o 3.00

Thickness: 1.878 GM/SQ CM θ 90.0

K Mev	$\frac{dn}{dK\,d\Omega}$ photon / Mev-ster-elect	$\frac{K}{Z^2}\frac{dn}{dK\,d\Omega}$ 1 / ster-electron	K Mev	$\frac{dn}{dK\,d\Omega}$ photon / Mev-ster-elect	$\frac{K}{Z^2}\frac{dn}{dK\,d\Omega}$ 1 / ster-electron
.05			1.55	.141 -3	.129 -5
.10	.236 -1	.140 -4	1.60	.120 -3	.114 -5
.15	.145 -1	.128 -4	1.65	.107 -3	.104 -5
.20	.911 -2	.108 -4	1.70	.923 -4	.928 -6
.25	.645 -2	.954 -5	1.75	.846 -4	.876 -6
.30	.436 -2	.773 -5	1.80	.687 -4	.732 -6
.35	.362 -2	.749 -5	1.85	.667 -4	.730 -6
.40	.298 -2	.705 -5	1.90	.470 -4	.528 -6
.45	.243 -2	.646 -5	1.95	.472 -4	.545 -6
.50	.204 -2	.603 -5	2.00	.332 -4	.393 -6
.55	.171 -2	.557 -5	2.05	.358 -4	.434 -6
.60	.147 -2	.523 -5	2.10	.215 -4	.267 -6
.65	.131 -2	.505 -5	2.15	.229 -4	.291 -6
.70	.113 -2	.466 -5	2.20	.204 -4	.265 -6
.75	.993 -3	.441 -5	2.25	.155 -4	.206 -6
.80	.873 -3	.413 -5	2.30	.107 -4	.146 -6
.85	.765 -3	.383 -5	2.35	.932 -5	.130 -6
.90	.660 -3	.352 -5	2.40	.998 -5	.142 -6
.95	.587 -3	.330 -5	2.45	.665 -5	.965 -7
1.00	.525 -3	.310 -5	2.50	.535 -5	.792 -7
1.05	.477 -3	.296 -5	2.55	.498 -5	.752 -7
1.10	.418 -3	.272 -5	2.60	.408 -5	.628 -7
1.15	.386 -3	.263 -5	2.65	.311 -5	.488 -7
1.20	.327 -3	.233 -5	2.70	.182 -5	.291 -7
1.25	.297 -3	.220 -5	2.75	.148 -5	.241 -7
1.30	.272 -3	.209 -5	2.80	.150 -5	.249 -7
1.35	.236 -3	.189 -5	2.85	.492 -6	.829 -8
1.40	.209 -3	.173 -5	2.90	.729 -6	.125 -7
1.45	.186 -3	.159 -5	2.95	.361 -6	.630 -8
1.50	.162 -3	.144 -5	3.00	.347 -6	.616 -8

TABLE 25

THICK TARGET BREMSSTRAHLUNG PRODUCTION

Material: ALUMINUM T_o 3.00

Thickness: 1.878 GM/SQ CM θ 120.0

K Mev	$\frac{dn}{dK\ d\Omega}$ photon / Mev-ster-elect	$\frac{K}{Z^2}\frac{dn}{dK\ d\Omega}$ 1 / ster-electron	K Mev	$\frac{dn}{dK\ d\Omega}$ photon / Mev-ster-elect	$\frac{K}{Z^2}\frac{dn}{dK\ d\Omega}$ 1 / ster-electron
.05			1.55	.501 -4	.460 -6
.10	.220 -1	.130 -4	1.60	.381 -4	.361 -6
.15	.141 -1	.125 -4	1.65	.319 -4	.311 -6
.20	.807 -2	.955 -5	1.70	.315 -4	.317 -6
.25	.529 -2	.782 -5	1.75	.235 -4	.244 -6
.30	.336 -2	.592 -5	1.80	.162 -4	.173 -6
.35	.253 -2	.524 -5	1.85	.171 -4	.186 -6
.40	.211 -2	.500 -5	1.90	.151 -4	.170 -6
.45	.165 -2	.439 -5	1.95	.113 -4	.130 -6
.50	.138 -2	.407 -5	2.00	.116 -4	.137 -6
.55	.108 -2	.352 -5	2.05	.913 -5	.111 -6
.60	.921 -3	.327 -5	2.10	.683 -5	.848 -7
.65	.781 -3	.300 -5	2.15	.633 -5	.806 -7
.70	.660 -3	.273 -5	2.20	.109 -4	.141 -6
.75	.546 -3	.242 -5	2.25	.220 -5	.293 -7
.80	.463 -3	.219 -5	2.30	.270 -5	.368 -7
.85	.414 -3	.207 -5	2.35	.299 -5	.416 -7
.90	.333 -3	.177 -5	2.40	.154 -5	.219 -7
.95	.307 -3	.173 -5	2.45	.883 -6	.128 -7
1.00	.252 -3	.149 -5	2.50	.784 -6	.116 -7
1.05	.207 -3	.128 -5	2.55	.729 -7	.110 -8
1.10	.192 -3	.125 -5	2.60	-.551 -6	-.847 -8
1.15	.165 -3	.112 -5	2.65	.154 -5	.241 -7
1.20	.145 -3	.998 -6	2.70	-.131 -6	-.209 -8
1.25	.117 -3	.868 -6	2.75	-.188 -5	-.305 -7
1.30	.103 -3	.795 -6	2.80	.927 -6	.154 -7
1.35	.903 -4	.721 -6	2.85		
1.40	.815 -4	.675 -6	2.90		
1.45	.640 -4	.549 -6	2.95		
1.50	.529 -4	.470 -6	3.00		